NATIONAL ADVISORY COMMITTEE FOR AERONAUTICS

TECHNICAL NOTE 3191

THEORETICAL INVESTIGATION OF LONGITUDINAL RESPONSE CHARACTERISTICS OF A SWEPT-WING FIGHTER AIRPLANE HAVING A NORMAL-ACCELERATION CONTROL SYSTEM AND A COMPARISON WITH OTHER TYPES OF SYSTEMS

By Fred H. Stokes and Charles W. Mathews

Langley Aeronautical Laboratory
Langley Field, Va.

Washington

July 1954

1C

NATIONAL ADVISORY COMMITTEE FOR AERONAUTICS

TECHNICAL NOTE 3191

THEORETICAL INVESTIGATION OF LONGITUDINAL RESPONSE CHARACTERISTICS OF A SWEPT-WING FIGHTER AIRPLANE HAVING A NORMAL-ACCELERATION CONTROL SYSTEM AND A COMPARISON WITH OTHER TYPES OF SYSTEMS

By Fred H. Stokes and Charles W. Mathews

SUMMARY

A theoretical investigation of the longitudinal response characteristics of a swept-wing fighter airplane using a normal-acceleration control system has been made. The system has been evaluated with normal-acceleration plus pitch-rate feedback and normal-acceleration plus pitch-rate feedback with a lag network placed in the forward loop. The effects of Mach number and altitude upon the response characteristics of the system and the effects of varying the parameter settings are determined. Also discussed are the elevator deflections and pitching velocities encountered at various parameter settings and flight conditions when an approximate step command in normal acceleration is impressed on the system. A comparison has been made between the normal-acceleration system and a pitch-attitude system when control of the flight path is desired, and, for further comparison, an angle-of-attack control and a pitch-rate control are discussed briefly.

Three primary conclusions were reached in this theoretical investigation: The airplane-autopilot combination incorporating both pitch-rate feedback and a lag network can be made to perform well as far as normal-acceleration response is concerned, for the flight conditions investigated, provided some means is available for changing the parameter settings. With the parameter settings which give the best response characteristics, the elevator deflections encountered at high altitudes and moderate to low speeds would be very large. Consequently, control-rate and control-deflection limitations, which are not considered in this paper, will have an important bearing on both the adjustment of parameters and the response of the system except for cases where commands are of small magnitude (such as might occur during the tracking phase of the attack of an automatic interceptor). When the pitch-attitude system and the normal-acceleration system were used as inner loops for controlling the flight path, the pitch-attitude system provided a more rapid flight-path response than did the normal-acceleration system.

INTRODUCTION

When automatic controls are added to the present-day high-speed fighter airplane, many possible variations are afforded as to how the airplane motions and loads can be controlled. The National Advisory Committee for Aeronautics has undertaken a theoretical investigation, the general purposes of which are (1) to study the response characteristics of an airplane having various types of longitudinal automatic-control-stabilization systems, such as pitch attitude, normal acceleration, and angle of attack, (2) to determine the effects of changes in altitude and Mach number on the response characteristics of the various systems, and (3) to determine the effects of changing the parameter settings on the response characteristics of the various systems. In the present paper, normal-acceleration stabilization and control is investigated and the effects on the performance of the airplane-autopilot combination of changing the flight conditions of the airplane and the parameter settings in the system are discussed. Results of a comparable study of a pitch-attitude stabilization and control system are presented in reference 1.

The types of controls analyzed herein incorporate normal-acceleration feedback alone, normal-acceleration plus pitch-rate feedback, and normal-acceleration plus pitch-rate feedback with a lag network placed in the forward loop.

The results presented are discussed on the basis of the characteristics of the frequency and transient response in normal acceleration, such as the frequency at which the peak-amplitude response occurs (hereinafter called the peak frequency), the time for the response to reach and stay within 5 percent of the steady-state value (hereinafter called the response time), the cycles to damp to one-half amplitude, and the steady-state error. A discussion is also presented of the elevator deflections and pitching velocities encountered at various parameter settings and flight conditions when an approximate step command in normal acceleration is impressed on the system. The normal-acceleration system and pitch-attitude system (ref. 1) are also compared when these two types of automatic control systems are used to control the flight path of the airplane.

Control systems sensing angle of attack and pitching velocity are also discussed briefly with particular regard to comparison of their characteristics with those of the normal-acceleration and pitch-attitude systems.

SYMBOLS

A	aspect ratio
a	time-constant ratio of lag network
b	wing span, ft
$C_{1/2}$	cycles for oscillations to damp to one-half amplitude
C_L	lift coefficient, L/qS
C_{L_α}	rate of change of lift coefficient with angle of attack, per radian
$C_{L_{\alpha_t}}$	rate of change of lift coefficient with angle of attack of tail, per radian
$C_{L_{D\theta}}$	rate of change of lift coefficient with nondimensional pitching velocity
$C_{L_{D\alpha}}$	rate of change of lift coefficient with rate of change of angle of attack
C_{L_δ}	rate of change of lift coefficient with elevator deflection, per radian
$C_{m_{C_L}}$	rate of change of pitching-moment coefficient with lift coefficient
C_{m_α}	rate of change of pitching-moment coefficient with angle of attack, per radian
$C_{m_{\alpha_t}}$	rate of change of pitching-moment coefficient with angle of attack of tail, per radian
$C_{m_{D\theta}}$	rate of change of pitching-moment coefficient with nondimensional pitching velocity
$C_{m_{D\alpha}}$	rate of change of pitching-moment coefficient with rate of change of angle of attack
C_{m_δ}	rate of change of pitching-moment coefficient with elevator deflection, per radian
$\bar{c}$	mean aerodynamic chord, ft

D	nondimensional differential operator, $\frac{\bar{c}}{V}\frac{d}{dt}$
g	acceleration due to gravity, ft/sec^2
h_p	pressure altitude, ft
I_Y	moment of inertia about Y-axis, slug-ft^2
$j = \sqrt{-1}$	
K_{n_ϵ}	normal-acceleration error-signal gain setting, radians per g
K_R	pitch-rate-signal gain setting, $\frac{\text{radians}}{\text{radians/sec}}$
K_Y	nondimensional radius of gyration about lateral stability axis
K_{γ_ϵ}	flight-path error-signal gain setting
L	lift, lb
l	tail length, measured from $0.25\bar{c}$ of wing to $0.25\bar{c}$ of tail, ft
M	Mach number; also pitching moment in figure 1
m	mass of airplane, slugs
n	normal acceleration, g units
p	complex Laplace operator
q	dynamic pressure, $\frac{1}{2}\rho V^2$, lb/sq ft
S	wing area, sq ft
T_R	time for response to reach and stay within 5 percent of steady-state value, sec
t	time, sec
V	airspeed, ft/sec
W	airplane weight, lb
X	longitudinal axis of reference fixed in airplane
Y_1	transfer function of elevator servocontrol system

Y_2	airplane transfer function relating pitch attitude to elevator deflection
Y_3	airplane transfer function relating normal acceleration to elevator deflection
Y_4	transfer function of lag network
Z	normal axis of reference fixed in airplane
α	angle of attack, radians
γ	angle of flight path with horizontal, radians
γ_ϵ	angle of flight-path error signal, $\gamma_i - \gamma_o$, radians
δ	elevator deflection, positive when trailing edge is down, radians unless otherwise specified
ϵ	error signal, $n_i - n_o$
ϵ_1	input to elevator servocontrol system
θ	angle of pitch, radians
Λ	angle of sweepback of 0.25-chord line, deg
μ	relative-density factor, $m/\rho S\bar{c}$
ρ	atmospheric density, slugs/cu ft
τ	lag-network time constant
Φ	phase angle, deg
ω	circular frequency, radians/sec
ω_p	frequency at which peak in amplitude response occurs, radians/sec
$d\epsilon/d\alpha$	rate of change of downwash with angle of attack
$\left\|n_o/n_i\right\|$	absolute value of amplitude ratio

Subscripts:

i	input
o	output
ss	steady state

A dot placed over a symbol indicates differentiation with respect to time.

ANALYSIS

The analysis of this paper was made by conventional techniques in which the concept of the transfer function was utilized. Thus, all the dynamic elements used in the analysis were assumed to have linear response characteristics. Although the elements of the system studied herein would, in all probability, exhibit nonlinear behavior under certain conditions, an investigation of these conditions is beyond the scope of this paper. An attempt is made, however, to point out where some of the more important nonlinearities might influence the results.

Airplane Transfer Function

The transfer function of the airplane relating normal acceleration to elevator deflection was obtained from an equation-of-motion type of analysis by use of stability derivatives estimated from theory, wind-tunnel data, and flight-test data. The various transfer functions used are presented in the appendix. The system of axes and the sign conventions used in deriving the airplane transfer functions are presented in figure 1. However, some sign conventions were modified for convenience in obtaining the response of the airplane-autopilot combination. The modification consisted of changing the sign of the numerator of the airplane transfer function which amounts, in effect, to considering the up elevator as positive. This modification is reasonable in that a positive elevator input will then produce a positive static response, a condition assumed to exist with most servo-synthesis procedures.

In the analysis, the degree of freedom involving changes in longitudinal velocity was neglected inasmuch as this paper is concerned primarily with short-period command characteristics.

Since the coefficients of the airplane transfer function vary with airspeed, altitude, Mach number, and other conditions, it is necessary

to study the control characteristics for flight conditions that represent the normal speed and altitude range of the airplane being considered. The four conditions selected were: condition I, $M = 0.5$ and $h_p = 35{,}000$ feet; condition II, $M = 0.7$ and $h_p = 0$; condition III, $M = 0.7$ and $h_p = 35{,}000$ feet; and condition IV, $M = 0.9$ and $h_p = 35{,}000$ feet. These flight conditions, the basic airplane dimensions, and the corresponding airplane stability parameters are presented in table I. The airplane and the flight conditions are the same as those studied in reference 1. Figure 2 shows the airplane frequency-response curves for the flight conditions investigated. These curves are in fairly good agreement with similar curves subsequently obtained from actual tests.

Transfer Function of Elevator Servocontrol System

The frequency response of the autopilot used throughout this analysis was obtained experimentally from a bench setup of a special autopilot system whose characteristics made it suitable for use in a high-speed fighter airplane. The autopilot considered (same as used in ref. 1) had essentially constant amplitude-response characteristics up to a frequency of about 6 cycles per second. The frequency response of this system is shown in figure 3, and a block diagram of the system is as follows:

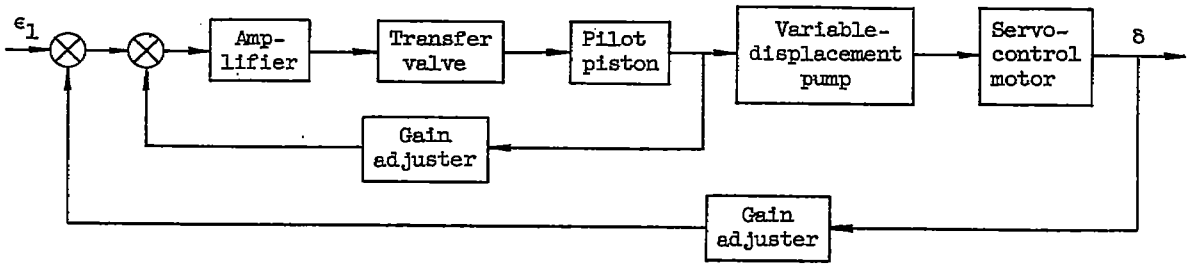

Airplane-Autopilot Combination

Initially the airplane-autopilot combination was investigated with the autopilot sensing acceleration errors only; however, pitch-rate feedback was incorporated throughout most of the investigations in order to improve the stability of the system and enable the use of higher system gains. In addition, a lag network was ultimately placed in the forward loop in order to reduce the large steady-state errors which

existed without the lag network. A block diagram of the airplane-autopilot combination with pitch-rate feedback and lag network is as follows:

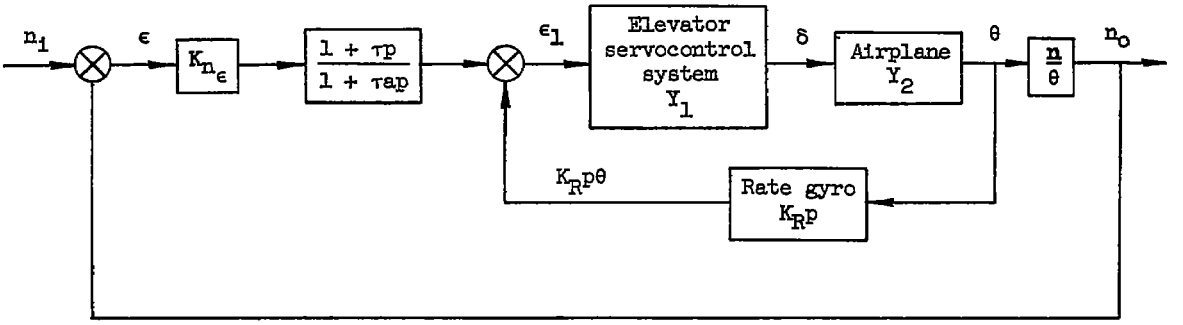

Dynamically, the feedback elements which measure normal acceleration and pitch rate were assumed to have an amplitude ratio of one and a phase lag of zero. The open- and closed-loop transfer functions of the systems analyzed are presented in the following table:

Type of system	Open loop n_o/ϵ	Closed loop n_o/n_i
Complete system	$\frac{K_{n_\epsilon} Y_1 Y_3 Y_4}{1 + K_R Y_1 Y_2 D}$	$\frac{K_{n_\epsilon} Y_1 Y_3 Y_4}{1 + K_R Y_1 Y_2 D + K_{n_\epsilon} Y_1 Y_3 Y_4}$
System without lag network	$\frac{K_{n_\epsilon} Y_1 Y_3}{1 + K_R Y_1 Y_2 D}$	$\frac{K_{n_\epsilon} Y_1 Y_3}{1 + K_R Y_1 Y_2 D + K_{n_\epsilon} Y_1 Y_3}$
System without pitch-rate feedback or lag network	$K_{n_\epsilon} Y_1 Y_3$	$\frac{K_{n_\epsilon} Y_1 Y_3}{1 + K_{n_\epsilon} Y_1 Y_3}$

where

Y_1 transfer function of elevator servocontrol system

Y_2 airplane transfer function relating pitch attitude to elevator deflection

Y_3 airplane transfer function relating normal acceleration to elevator deflection

Y_4 lag-network transfer function, $\frac{1 + \tau p}{1 + \tau a p}$

The procedure used in establishing the parameter settings K_R, K_{n_ϵ}, τ, and a for the complete system is as follows: The gain settings K_R and K_{n_ϵ} were initially determined by a well-known technique which involved adjusting the peak amplitude ratio of the closed loop (see ref. 2, pp. 185 to 188). At each flight condition investigated, the gain setting K_R was determined so that the peak amplitude ratio of the inner loop was adjusted to a value of approximately 1.2. Then, the error gain setting K_{n_ϵ} was determined in a similar manner so that the peak amplitude ratio of the outer loop was also adjusted to a value of approximately 1.2. At this point, it should be noted that, for the normal-acceleration systems investigated, a unit static sensitivity was not achieved. Thus, the degree of stability of these systems is more directly related to the ratio of the peak amplitude ratio to the static-amplitude ratio than to the peak amplitude ratio itself. Because a close approach to a static-amplitude ratio of one was desired, however, combinations having low static-amplitude ratios were not of interest and, therefore, adjustment to a given peak amplitude ratio was justified. For the normal-acceleration system investigated with the best gain adjustments at each flight condition, the static-amplitude ratios obtained when the peak amplitude ratio was adjusted to 1.2, resulted in ratios of peak amplitude ratio to static-amplitude ratio which varied from 1.4 to 1.7. Variations of this magnitude would be expected to have but little effect on the transient-response characteristics of the system. Further refinement in adjusting the characteristics of the outer loop was not felt to be warranted in the absence of a more definite criterion on the relative importance of such factors as steady-state error, response time, and the degree of system stability.

The values of the lag-network variables τ and a were determined from Nyquist plots of the system without the lag network. M-circles were superimposed on the plots to determine the frequency range over which an integrating characteristic was required. After incorporating the lag network, K_{n_ϵ} was readjusted to maintain a peak amplitude ratio at the

value selected. In order to verify that the values of the parameters obtained by the technique just described were near the best values for the chosen system, the effects of altering the parameter settings were investigated. While the other settings were held constant, each parameter setting was decreased and increased by 50 percent of its original value. At the same time, K_{n_ϵ} was changed to maintain a peak amplitude ratio at the value selected. In this manner, the trend of the frequency-response curves could be seen. In addition to varying the parameter settings in order to determine their effects on the frequency and transient responses, the effects of holding the system parameter settings constant while varying the flight condition were investigated. Initially, the parameter settings which gave the best results at the altitude cruising condition, condition III ($M = 0.7$, $h_p = 35{,}000$ feet), were used and, finally, the parameter settings which gave the best results at the sea-level condition, condition II ($M = 0.7$, $h_p = 0$), were used. As mentioned previously, the values of system parameters were chosen by techniques applicable only to linear systems. The gain settings so obtained were large compared to those currently considered for use in this type of control system (particularly for high altitudes at low to moderate speeds). The use of lower gains may be dictated by considerations of control-deflection limitations and control-rate limitations. It should be pointed out that gains which gave the best results at sea level were much lower than those determined for high altitudes. Since operation at high altitude with the sea-level gain settings was investigated, effects on the system response of operating with reduced gains are included in the present study.

The Fourier synthesizer, the type described in reference 3, was employed to establish the transient-response characteristics for all the systems analyzed from their closed-loop frequency response. The input quantity, normal-acceleration command n_1, was in the form of an approximate square wave utilizing the first 24 harmonics of a Fourier series (see fig. 4).

The response characteristics that were used to evaluate the various conditions were (1) the peak frequency ω_p, (2) the response time T_R, (3) the number of cycles to damp to one-half amplitude $C_{1/2}$, and (4) the steady-state error ϵ_{ss}. In addition to obtaining the transient responses in normal acceleration, calculations were also made of the elevator deflections needed to produce these responses and of the pitching velocities encountered when the system was subjected to the normal-acceleration command. Expressions for the transfer functions δ/n_1 and $\dot{\theta}/n_1$ are presented in the appendix. These relations were employed to determine the associated transient-response characteristics through use of the Fourier synthesizer. The elevator deflections and pitching

velocities were investigated at all four flight conditions with the best parameter settings obtained at each condition, with the parameter settings held constant throughout all conditions at the best values obtained for the high-altitude cruising conditions, and with the parameter settings held constant throughout all conditions at the best values obtained for the sea-level condition.

Normal-Acceleration Autopilot As a Command System for Control of the Flight Path

A typical application of the normal-acceleration airplane-autopilot combination is to control the flight path of the airplane. A block diagram of such a system is as follows:

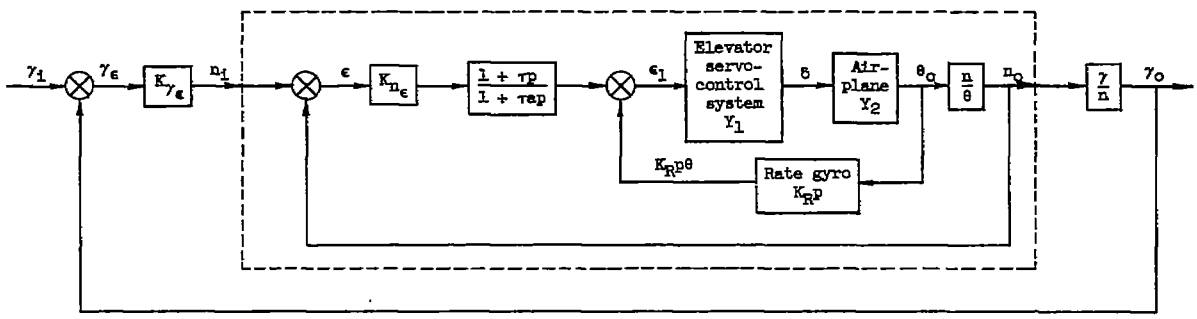

The open-loop transfer function appears symbolically as

$$\frac{\gamma_o}{\gamma_\epsilon} = K_{\gamma_\epsilon} \frac{n_o}{n_i} \frac{\gamma}{n}$$

The parameter settings used in evaluating this system were the best settings obtained at each flight condition of the normal-acceleration airplane-autopilot combination which utilized both the rate-gyro and lag-network systems. When these parameter settings were used, the transient responses of the system at all four flight conditions were determined. In addition to obtaining the transient responses in flight path, calculations were also made of the elevator deflections needed to produce these responses and of the normal acceleration imposed upon the airframe when the system was subjected to the flight-path command. Expressions for the transfer functions γ_o/γ_i, δ/γ_i, and n/γ_i are presented in the appendix.

RESULTS AND DISCUSSION

Airplane-Autopilot Combination Without Pitch-Rate Feedback or Lag Network

The best frequency and transient responses obtained for the system without pitch-rate feedback or lag network are shown in figure 5 for all four flight conditions. The approximate square-wave input produced by the Fourier synthesizer is also plotted for comparison. For simplicity, this input curve in figure 5 and in subsequent figures was smoothed so that the ripples existing in the actual input (see fig. 4) would not appear. The fairing of this curve was justified because the frequency of the ripples was high enough to have no significant effect on the output; small ripples were caused by the limited number of harmonics utilized by the Fourier synthesizer. In addition, the parameters ω_p, T_R, $C_{1/2}$, and ϵ_{ss} which are associated with each frequency and transient response are tabulated in figure 5. Note that the acceleration transients in figure 5 and subsequent figures initially tend to go in the opposite direction from the command. This condition results from the fact that the initial change in tail load with elevator deflection produces an acceleration opposite to that ultimately obtained in the steady state.

It is obvious from figure 5 that, for all four flight conditions, the dynamic characteristics of the airplane-autopilot would be unsatisfactory because of the long time required for the airplane to respond to an applied command, the very low damping of the system, and the large steady-state error. Improvement in the transient response could be effected by increasing both the amplitude ratio at the low-frequency end of the frequency-response curves and the peak frequency without increasing the peak amplitude ratio of the curves. As is well known, the addition of derivative feedback would make it possible to accomplish this purpose.

Airplane-Autopilot Combination With Pitch-Rate Feedback Withoug Lag Network

The frequency and transient responses obtained with pitch-rate feedback incorporated for the four flight conditions are presented in figure 6. A comparison of figure 5 with figure 6 shows that the addition of pitch-rate feedback improved the system inasmuch as the static value of the frequency response was increased, the peak frequency was increased, and the response time was decreased. Even though the system

was improved with the addition of pitch-rate feedback, the amplitude ratio at the low-frequency end of the frequency-response curve did not increase sufficiently to afford the attainment of a reasonably small steady-state error. Therefore, in order to increase the amplitude ratio at the low-frequency end of the frequency-response curve and lower the steady-state error, a lag network was incorporated in the system.

With the assumed static margin, a steady-state error will always exist when the autopilot is operated by the acceleration error alone. The $C_{m_{C_L}}$ values for the example airplane presented in table I show that, for the flight conditions investigated, the airplane had a fairly large static margin. Reduction in the static margin would reduce the steady-state errors obtained herein. In fact, for approximately zero static margin, an integrating characteristic would exist in the airplane transfer function. This consideration and others, such as the magnitude of elevator deflection to obtain a given response, indicate the desirability of operating with low static margins when under automatic control.

Airplane-Autopilot Combination With Both Pitch-Rate Feedback and Lag Network

The frequency and transient responses obtained with both pitch-rate feedback and a lag network incorporated in the system are presented in figure 7. Results are shown for all four flight conditions when the best parameter settings obtained were used. These settings were obtained by examining the trends in the response curves as the system parameters were varied. Typical effects of varying system parameters are presented in figures 8 to 13. The original parameter settings (middle row of figs. 8 to 13) are not necessarily the best settings. A comparison of figure 7 with figure 6 shows that, for all four flight conditions, the amplitude ratio of the frequency-response curve at low frequencies was greatly increased and, as a result, there was a sizeable decrease in the steady-state error. If perfect integration had been provided by the lag network, the steady-state error could have been reduced to zero for all conditions; however, because of the appearance of a secondary peak at low frequency, it was necessary to select a lag network which would not continue to increase the gain all the way to zero frequency. With the network chosen, the usable error gains increased sharply at each flight condition because of the attenuation at high frequencies afforded by this lag network. The peak frequency of the frequency-response curves decreased somewhat, but the large increases in amplitude ratio at frequencies below the peak more than offset the adverse effect of this decrease. Thus, the results presented in figure 7 indicate that the

present airplane-autopilot combination can be made to have a very rapid normal-acceleration response, provided some means of changing the parameter settings is available.

Effects of Varying the Parameter Settings

In figures 8 to 13, the original parameter settings were determined by the procedures outlined in the analysis. Only conditions II ($M = 0.7$, $h_p = 0$) and III ($M = 0.7$, $h_p = 35{,}000$ feet) were used to illustrate the effects of varying the parameter settings since the other conditions were found to produce similar results. For the purpose of determining the effects of variations in the parameter settings, the original values of the parameter settings were (1) decreased by 50 percent and (2) increased by 50 percent while the peak-amplitude ratio of the outer loop was maintained constant. The results obtained with these changes in parameter settings are presented in figures 8 to 13. This original case corresponds to the middle row in each figure. For perfect following, the amplitude response would have a value of unity from zero to infinite frequency and the phase-angle curve would be zero for all values of ω. This result obviously is impossible to achieve in practice, but any modification which serves to increase the peak frequency ω_p or increase the magnitude at low frequencies of the frequency-response curve without encountering a high peak amplitude ratio makes possible a closer approach to this ideal curve. Similarly, inasmuch as perfect following would involve no phase lag, any modification that generally reduces the phase-angle variation with frequency would improve the response.

Figures 8 and 11 show the results of the airplane-autopilot combination with both pitch-rate feedback and lag network when the pitch-rate gain is altered by ±50 percent of its original value for conditions II and III for the sea-level and altitude conditions at $M = 0.7$. In both figures, it is readily apparent that an increase in pitch-rate gain increases the peak frequency and makes possible an increase in error gain to a limited extent. Too much of an increase in pitch-rate gain lowers the amplitude ratio of the frequency-response curve at frequencies below the peak frequency and thereby makes the response sluggish. Altering the pitch-rate-gain setting did not appreciably affect the static value of the frequency-response curve.

The response time exhibited moderate increases when the pitch-rate gain was increased by 50 percent, and a decrease of 50 percent in pitch-rate gain setting increased the response time considerably. The effects of changes in pitch-rate gain settings on the stability of the system in terms of $C_{1/2}$ was more pronounced than the effect on T_R.

The results obtained when the lag-network time constant τ was altered are presented in figures 9 and 12. Actually, the reciprocal of the time constant, the break frequency, was the parameter that was varied by ±50 percent since the analysis was done in the frequency domain. When the break frequency was altered in this manner, τ was doubled and then reduced by two-thirds of its original value. As the time constant was increased (the break frequency being decreased by 50 percent), the peak frequency increased. The figures indicate that there was a more pronounced effect on the peak frequency for a 50-percent increase in break frequency than for a 50-percent decrease in break frequency. The response characteristics T_R, $C_{1/2}$, and ϵ_{ss} did not change appreciably when the time constant τ was altered, but this result was obtained with the ratio of the time constants of the lag network held fixed which in turn fixed the ratio of the low-to-high frequency gain of the lag network.

Figures 10 and 13 present the results obtained when the time-constant ratio of lag network a was increased and decreased by 50 percent of its original value. These figures indicate that an increase in the time-constant ratio decreases the peak frequency but increases the error gain setting of the system. Since the error gain setting increased with an increase in a, the percentage of steady-state error ϵ_{ss} decreased because ϵ_{ss} is directly dependent upon the error gain setting. It is obvious from figures 10 and 13 that the time-constant ratio affects the low-frequency end of the frequency-response curve but has little effect at high frequencies. Neither the response time T_R nor the stability of the systems in terms of $C_{1/2}$ was significantly altered with a ±50 percent change in the time-constant ratio. Although there was a sizeable decrease in steady-state error as the time-constant ratio was increased, the magnitude of this ratio was limited by the appearance of another peak in the frequency-response curve at fairly low frequencies. This tendency toward a low-frequency peak can be detected in some of the frequency-response curves presented in figures 10 and 13.

Effects of Mach Number and Altitude

The variation of the parameter settings with flight conditions is necessitated by the alterations in the airplane frequency response (as shown in fig. 2). The effects of change in Mach number at a constant altitude (35,000 feet) can be seen by comparing conditions I, III, and IV (Mach numbers of 0.5, 0.7, and 0.9, respectively) of figure 7. Figure 7 presents the results of the four flight conditions investigated when the best parameter settings obtained at each condition are used. As the Mach number is increased from 0.5 to 0.9, the gain settings decrease in magnitude by a factor of about 2.5 while the lag-network

settings change only slightly. This decrease in gain settings is made possible because, at subsonic speeds, the frequency response of the airplane usually improves with increased airspeed. A point worth noting, however, is that, with the best parameter settings obtained at each high-altitude condition (fig. 7), the response time and degree of stability of the airplane-autopilot combination correspond closely for all the flight conditions investigated. Since the lag-network settings τ and a change only slightly with an increase in Mach number, there is an indication that these settings could be held constant with changes in Mach number.

A comparison of conditions II and III of figure 7 (altitudes of sea level and 35,000 feet, respectively) shows the effects of altitude change at constant Mach number (M = 0.7). In going from sea level to an altitude of 35,000 feet, the best pitch-rate gain setting obtained increased by a factor of about 4 while the best error gain setting obtained increased by a factor of about 7. The parameter settings of the lag network decreased only slightly; this decrease indicated that constant settings may be used for the lag network when either the altitude or Mach number are changed. The necessity for the increase in pitch-rate gain and error gain settings with increase in operating altitude can be seen by comparing the airplane frequency-response curves for the two altitudes investigated (see fig. 2). The response characteristics of the airplane are much better at lower altitude. A more detailed discussion of the effect of altitude on the airplane response is contained in reference 1.

The analysis thus far has shown that the parameter settings of the airplane-autopilot combination with both pitch-rate feedback and lag network can be adjusted to give high performance at each flight condition; however, a simpler automatic system would result if parameter settings could be held constant through the Mach number and altitude ranges. The effects of holding the parameter settings constant while varying the flight conditions were investigated and the results are shown in figures 14 and 15. In figure 14, the parameter settings that were chosen were the best parameter settings obtained for the altitude cruising condition (see fig. 7). The system became unstable at conditions II (M = 0.7, h_p = 0) and IV (M = 0.9, h_p = 35,000 feet) whereas at condition I (M = 0.5, h_p = 35,000 feet) there was a large increase in response time. In the case of conditions II and IV, the large pitch-rate gain (compare best pitch-rate gains of figs. 7 and 14) caused the inner loop of the system to become unstable. The system became sluggish for condition I because of the substantial decrease in error gain.

In figure 15, the parameter settings that were held constant as the flight conditions were varied were the best parameter settings obtained for the sea-level condition (see second row of fig. 7). All the flight

conditions in this figure are stable. At the altitude conditions, the system became very sluggish but improved as the Mach number was increased. This response resulted from the low gain settings K_R and K_{n_ϵ} obtained at the sea-level condition in comparison with the best gain settings obtained at altitude; however, there is still the possibility of operating the normal-acceleration airplane-autopilot combination by using a compromise of gain settings provided it is established that a much slower response can be tolerated than the best response obtained for each condition.

Elevator Deflections and Pitching Velocities

The response characteristics of the basic controlled quantity, in this case normal acceleration, do not alone determine the adequacy of a given system. The control motions are important in determining the effects on the maximum rate, force, and power output of the servomotor. In addition, the pitching motion may be important.

Because of these aspects, the elevator deflections and the pitching velocities in response to the approximate step command in normal acceleration were investigated for each flight condition. The results obtained when the best parameter settings at each flight condition were used are presented in figure 16.

The magnitudes of the elevator deflections at their initial peaks are somewhat under the value expected from the error gain setting. Since the ratio $\delta/[n_i]_{ss}$ has the units of degrees per g, it is necessary to divide the control deflections in figure 16 by 57.3 so that both the quantities $\delta/[n_i]_{ss}$ and K_{n_ϵ} are in the same units. For an input of the abruptness shown, these ratios indicate that for conditions I ($M = 0.5$, $h_p = 35{,}000$ feet) and III ($M = 0.7$, $h_p = 35{,}000$ feet), the control rates and deflections are very high. Consequently, control-rate and control-deflection limitations, which are not considered herein, will have important effects on the response except for commands of small magnitude. The pitching velocities as plotted in figure 16 are within reasonable limits for conditions II ($M = 0.7$, $h_p = 0$) and IV ($M = 0.9$, $h_p = 35{,}000$ feet), but the magnitudes for conditions I and III are large. The magnitudes at all four flight conditions could be reduced at the expense of the response, if it were established that a poorer response could be tolerated.

The details of the pitching velocities in response to a normal-acceleration command are of interest in that they afford some insight into the characteristics of a pitching-velocity command system as compared with a normal-acceleration command system. The time histories of

pitching velocity show that its peak values attained in response to an acceleration command are many times the values ultimately attained in the steady state. This observation leads to the conclusion that if a pitching-velocity command system were optimized to have the pitching-velocity response follow a step command as closely as possible, the normal-acceleration response to a pitching-velocity command would tend to be quite sluggish. In applying these command systems to control the flight path of an airplane, the impression is gained that the normal-acceleration command system would be superior, since the rate of change of the flight path is directly proportional to the normal acceleration and, as pointed out, the transient-response characteristics in normal acceleration would be much superior for the normal-acceleration command system than for the pitching-velocity command system.

The elevator deflections and pitching velocities in response to normal-acceleration commands were also obtained for the cases where the autopilot parameter settings were held constant and the flight conditions varied. The effects on the normal-acceleration response have been presented in figures 14 and 15. The chief observation relative to the elevator deflections and pitching velocities is that the peak values of these quantities were of the same order of magnitude for all flight conditions investigated when the parameter settings were fixed. When the sea-level settings (see fig. 16) were used, the peak values were not usually large, being about 3 degrees per g for elevator deflections and about 0.2 radian per second per g of pitching velocities.

Comparison of Normal-Acceleration and Pitch-Attitude Systems When Used To Control Flight Path

As implied previously herein and as pointed out in reference 1, often the purpose of a command system is to provide control of some quantity other than the basic quantity. In particular, various types of command systems are used to control the flight path of an airplane. Accordingly, the use of a pitch-attitude command system to control the flight path was discussed in reference 1. As pointed out therein, a pitch-attitude system with no external-path loop affords control of the flight path since there is a one-to-one correspondence between the flight-path angle and pitch-attitude angle of an airplane in the steady state; however, under these conditions, the flight-path response tended to be sluggish even with an extremely rapid attitude response. In order to use a normal-acceleration command system for control of the flight path, a modification must be made to make the system sensitive to the flight path itself, since a steady normal acceleration of an airplane produces a steady rate of change of flight path. This modification can

be accomplished by adding an outer loop sensitive to flight path and producing an acceleration command proportional to the error between the desired and existing flight-path angle. Such a modification could also be made to a pitch-attitude command system and the flight-path responses might thereby be improved over those presented in reference 1. Expressions for the transfer functions γ_o/γ_i, δ/γ_i, and n/γ_i, when using the pitch-attitude system, are the same as those presented in the appendix for the normal-acceleration system except that the θ_o/θ_i transfer function presented in reference 1 is substituted for the n_o/n_i transfer function.

Figures 17 and 18 present the flight-path response, elevator deflections, and normal accelerations encountered when the normal-acceleration system considered herein (fig. 17) and the pitch-attitude system considered in reference 1 (fig. 18) are used as an inner loop in a flight-path control system. Both figures indicate that the flight-path responses are slow in comparison with those obtained in the normal-acceleration system or the pitch-attitude system but are considerably improved over the path responses obtained in reference 1. The elevator deflections are very rapid. In most instances, the elevator deflections have undergone a large amplitude pulse before significant path responses have occurred and also have nearly steadied out as the flight-path response reaches its initial peak. The magnitude of the elevator deflections for altitude conditions I, III, and IV are high, but the normal accelerations produced by these deflections are not particularly large because of the high frequencies involved in the elevator motion.

A comparison of the flight-path responses in figures 17 and 18 indicates certain important differences between use of the normal-acceleration system and the pitch-attitude system as an inner loop in a flight-path control system. The flight-path responses are more rapid for the pitch-attitude system than for the normal-acceleration system and reflect a significantly higher peak frequency for a given peak magnification of the outer loop for the pitch-attitude system. This better transient response for the pitch-attitude system stems from the better frequency-response characteristics (particularly in phase) obtained for the attitude command system than those which were obtained for the normal-acceleration command system. In addition, the airplane transfer function relating flight path to attitude has somewhat better phase characteristics than the airplane transfer function relating flight path to normal acceleration. On the other hand, because the airplane transfer function γ/θ does not have an integrating characteristic as does the transfer function γ/n, the flight-path response using the pitch-attitude system does have a steady-state error. The ability to maintain steady-state errors as low as those shown in figure 18 is dependent on the ability to obtain a pitch-attitude command system with as high a performance as was obtained for the one examined in reference 1.

The magnitude of the elevator deflections are much less when the normal-acceleration system is utilized, and this fact also may be a consideration in selecting the type of command control system.

Comparison of Pitch-Attitude and Normal-Acceleration Systems With a System Which Controls Angle of Attack

Another important variable in the longitudinal motion is angle of attack. Automatic control of this quantity may be desirable under several flight conditions, in particular, during landings where a safe margin below the stall angle of attack is desired and during cruising where angle of attack is a primary variable in the determination of range performance. As with the normal-acceleration and pitch-attitude autopilots, an angle-of-attack autopilot might also be used as an inner loop in the control of some other quantity such as flight path. Inclusion of the study of an angle-of-attack autopilot in a general survey of longitudinal-control systems, therefore, is desirable.

Early in the analysis of an angle-of-attack system, certain similarities between it and the pitch-attitude system became apparent; therefore, further analysis of the angle-of-attack system was obviated. This similarity can be attributed directly to the airplane transfer functions which involve pitch attitude and angle of attack. For comparison, these transfer functions are plotted in figure 19 for the example airplane used in the analysis at a Mach number of 0.7 and an altitude of 35,000 feet and, in terms of the airplane stability derivatives, are as follows:

$$\frac{\theta}{\delta} = \frac{\left(C_{m_\delta}C_{L_{D\alpha}} - C_{m_{D\alpha}}C_{L_\delta} + 2\mu C_{m_\delta}\right)D + C_{L_\alpha}C_{m_\delta} - C_{m_\alpha}C_{L_\delta}}{\left(2\mu K_Y{}^2C_{L_{D\alpha}} + 4\mu^2K_Y{}^2\right)D^3 + \left(-2\mu C_{m_{D\alpha}} + C_{L_{D\theta}}C_{m_{D\alpha}} - 2\mu C_{m_{D\theta}} + 2\mu K_Y{}^2C_{L_\alpha} - C_{m_{D\theta}}C_{L_{D\alpha}}\right)D^2 + \left(-2\mu C_{m_\alpha} + C_{m_\alpha}C_{L_{D\theta}} - C_{L_\alpha}C_{m_{D\theta}}\right)D}$$

$$\frac{\alpha}{\delta} = \frac{\left(-2\mu K_Y{}^2C_{L_\delta}\right)D + 2\mu C_{m_\delta} - C_{m_\delta}C_{L_{D\theta}} + C_{L_\delta}C_{m_{D\theta}}}{\left(2\mu K_Y{}^2C_{L_{D\alpha}} + 4\mu^2K_Y{}^2\right)D^2 + \left(-2\mu C_{m_{D\alpha}} + C_{L_{D\theta}}C_{m_{D\alpha}} - 2\mu C_{m_{D\theta}} + 2\mu K_Y{}^2C_{L_\alpha} - C_{m_{D\theta}}C_{L_{D\alpha}}\right)D + \left(-2\mu C_{m_\alpha} + C_{m_\alpha}C_{L_{D\theta}} - C_{L_\alpha}C_{m_{D\theta}}\right)}$$

The two frequency responses are substantially the same over a large range of intermediate frequencies. This similarity results from the dominance of the term $2\mu C_{m_\delta}$ in the numerator of both transfer functions. For the angle-of-attack transfer function (in the case of the example airplane), the $2\mu C_{m_\delta}$ terms are of an order of magnitude greater than all others at frequencies above 5 radians per second, and, for the pitch-attitude transfer function, this term is of an order of magnitude greater than all

others at frequencies below about 100 radians per second. The discrepancies between the two transfer functions at large frequencies is unimportant since the airplane response is so attenuated as not to affect the response characteristics of the airplane-autopilot combination. Of course, the lack of a low-frequency integrating characteristic in the case of the angle-of-attack transfer function is important, but such a characteristic can be provided by incorporating a lag network of the form $\frac{1 + \tau p}{\tau p}$ in the complete system. With this addition, the transfer function of the complete system for controlling angle of attack can be made about the same over the important range of frequencies as obtained for the system which controls pitch attitude. This result may be seen from the plots presented in figure 20 for the transfer functions of the angle-of-attack and pitch-attitude airplane-autopilot combinations. The magnitudes of pitch-rate gain and error gain for the best response were found to be practically the same for both systems. Actually, it was found possible to provide a somewhat better integrating characteristic in the system through use of a lag network than was inherent in the airplane in the case of the pitch-attitude system, but this difference did not materially affect the similarity of the transient-response characteristics of the two systems. The general conclusion to be derived from these observations is that the results for the pitch-attitude systems presented in reference 1 and in this paper are, in general, directly applicable to an angle-of-attack system, provided an integrating characteristic is incorporated in the angle-of-attack autopilot.

CONCLUSIONS

A theoretical analysis has been made of the longitudinal response characteristics of a swept-wing fighter airplane having a normal-acceleration control system. The effects of varying the parameter settings of the system and the airplane flight conditions were investigated. Results are applicable to the range of conditions in which the system exhibits linear behavior. Therefore, the responses obtained are believed to be considerably better than could be obtained under many conditions because of the detrimental effect of such nonlinearities as control-displacement limitations and control-rate limitations. The results do apply directly when commands are of small magnitude (such as might occur during the tracking phase of the attack of an automatic interceptor). From this analysis the following conclusions were reached:

1. When the frequency responses and transient responses of the normal-acceleration system with normal-acceleration feedback alone were analyzed, the error gains were limited to low values of all flight conditions by consideration of system stability. As a result, the response in normal acceleration was sluggish and large steady-state errors occurred.

When the system incorporated both a pitch-rate gyro and a lag network in the forward loop, very rapid responses could be made provided that some means was available of changing the gain settings with flight conditions.

2. The normal-acceleration system was fairly sensitive to changes in pitch-rate gain. A 50-percent change significantly affected the stability of the system, the response time, and the steady-state error.

3. An increase in Mach number from 0.5 to 0.9 at an altitude of 35,000 feet decreased the magnitude of the gain settings for the best response characteristics by a factor of about 2.5. This reduction was brought about by a general improvement in the airplane frequency response with increase in airspeed in the subsonic speed range. Similar effects resulted from decreasing altitude at a constant Mach number.

4. In view of the fact that the lag-network parameter settings T and a retained approximately the same magnitude at each flight condition, it is concluded that these parameters could be held constant throughout the flight conditions investigated.

5. At a Mach number of 0.7 at sea level or at a Mach number of 0.9 at high altitudes, with the best parameter settings obtained for cruising speeds at high altitudes being used, the system became unstable. At high altitude, with the best parameter settings obtained for the sea-level condition, there was a general trend toward improved stability but a much more sluggish response.

6. If a pitching-velocity command system were optimized to have the pitching-velocity response follow a command as closely as possible, the normal-acceleration response obtained with the pitching-velocity system would tend to be quite sluggish as compared with the normal-acceleration response obtained with the normal-acceleration system. In applying these command systems to control the flight path of an airplane, the impression is therefore gained that the normal-acceleration command system would be superior.

7. When the pitch-attitude system considered in NACA TN 2882 and the normal-acceleration system considered herein were used as inner loops for controlling the flight path of the airplane, the pitch-attitude system showed a more rapid flight-path response than did the normal-acceleration system, but the pitch-attitude system exhibited a steady-state error.

8. A preliminary analysis of an angle-of-attack system indicated that its characteristics, both as a command system for control of angle of attack or as an inner loop for control of some other quantity, would be practically the same as for a pitch-attitude system provided an integrating characteristic is incorporated in the angle-of-attack autopilot.

9. For all systems studied, very high gains were utilized, particularly for the high altitudes at moderate to low speeds. As a result, the elevator rates and deflections were very high, and, in the practical application of such systems, the effects of factors such as control-rate and control-deflection limitations would have to be considered.

Langley Aeronautical Laboratory,
National Advisory Committee for Aeronautics,
Langley Field, Va., March 8, 1954.

APPENDIX

TRANSFER FUNCTIONS APPLICABLE TO PRESENT ANALYSIS

The longitudinal equations of motion in nondimensional form used in the analysis are

$$\left(2\mu K_Y^2 D - C_{m_{D\theta}}\right)D\theta + \left(-C_{m_\alpha} - C_{m_{D\alpha}}D\right)\alpha = C_{m_\delta}\delta \tag{1}$$

$$\left(2\mu - C_{L_{D\theta}}\right)D\theta + \left(-2\mu D - C_{L_\alpha} - C_{L_{D\alpha}}D\right)\alpha = C_{L_\delta}\delta \tag{2}$$

The transfer function of the airplane that relates normal-acceleration to elevator-deflection input in terms of airplane stability derivatives, as derived from equations (1) and (2) and the expression

$$n = \frac{V^2}{g\bar{c}}(D\theta - D\alpha) = \frac{V^2}{g\bar{c}}D\gamma \tag{3}$$

is of the form:

$$\frac{n}{\delta} = \frac{V^2}{g\bar{c}}\left(\frac{AD^2 + BD + C}{ED^2 + FD + G}\right)$$

where

$$A = 2\mu K_Y^2 C_{L_\delta}$$

$$B = C_{m_\delta}C_{L_{D\theta}} - C_{L_\delta}C_{m_{D\theta}} + C_{m_\delta}C_{L_{D\alpha}} - C_{m_{D\alpha}}C_{L_\delta}$$

$$C = -C_{m_\alpha}C_{L_\delta} + C_{L_\alpha}C_{m_\delta}$$

$$E = 2\mu K_Y^2 C_{L_{D\alpha}} + 4\mu^2 K_Y^2$$

$$F = -2\mu C_{m_{D\alpha}} + C_{L_{D\theta}}C_{m_{D\alpha}} - 2\mu C_{m_{D\theta}} + 2\mu K_Y^2 C_{L_\alpha} - C_{m_{D\theta}}C_{L_{D\alpha}}$$

$$G = -2\mu C_{m_\alpha} + C_{m_\alpha}C_{L_{D\theta}} - C_{L_\alpha}C_{m_{D\theta}}$$

The dimensionalized form of the n/δ transfer function may be obtained by substituting $\frac{\bar{c}}{V}p$ for D. Then the n/δ transfer function becomes

$$\frac{n}{\delta} = \frac{V^2}{g\bar{c}}\left[\frac{A\left(\frac{\bar{c}}{V}\right)^2 p^2 + B\left(\frac{\bar{c}}{V}\right)p + C}{E\left(\frac{\bar{c}}{V}\right)^2 p^2 + F\left(\frac{\bar{c}}{V}\right)p + G}\right]$$

The frequency-response form of the dimensionalized transfer function may be obtained by substituting $j\omega$ for the Laplace operator p.

The transfer function of the airplane relating angle of attack to elevator deflection can also be derived from equations (1) and (2) and is of the form

$$\frac{\alpha}{\delta} = \frac{PD + Q}{ED^2 + FD + G}$$

where

$$P = -2\mu K_Y{}^2 C_{L_\delta}$$

$$Q = 2\mu C_{m_\delta} - C_{m_\delta} C_{L_{D\theta}} + C_{L_\delta} C_{m_{D\theta}}$$

The dimensionalized form of the α/δ transfer function may be obtained by substituting $\frac{\bar{c}}{V}p$ for D. Then the α/δ transfer function becomes

$$\frac{\alpha}{\delta} = \frac{P\left(\frac{\bar{c}}{V}\right)p + Q}{E\left(\frac{\bar{c}}{V}\right)^2 p^2 + F\left(\frac{\bar{c}}{V}\right)p + G}$$

A block diagram of the normal-acceleration command system considered is presented in the analysis. The open-loop transfer function of this system is

$$\frac{n_o}{\epsilon} = \frac{K_{n_\epsilon} Y_1 Y_3 Y_4}{1 + K_R Y_1 Y_2 D}$$

where Y_1 is the autopilot transfer function, Y_2 is the airplane transfer function relating pitch attitude to elevator deflection, Y_3 is the airplane transfer function relating normal acceleration to elevator deflection, and Y_4 is the lag-network transfer function. The closed-loop transfer function of the system is

$$\frac{n_o}{n_i} = \frac{\frac{n_o}{\epsilon}}{1 + \frac{n_o}{\epsilon}}$$

The known transfer functions of the airplane, the autopilot, and the lag network, together with the selected parameter settings, were used to find the frequency response of the closed-loop transfer function of the system. The frequency-response data were fed into the Fourier synthesizer to determine the transient-response characteristics of the system.

The transfer function relating elevator deflection to the normal-acceleration input command of the closed-loop system was obtained from the airplane transfer function relating normal acceleration to elevator deflection (previously defined) and from the closed-loop transfer function of the system relating normal-acceleration output to the normal-acceleration input command. Thus,

$$\frac{\delta}{n_i} = \frac{n_o/n_i}{n_o/\delta}$$

In a similar manner, the transfer function relating pitch attitude to elevator deflection (see ref. 3) was used to establish the transfer functions relating pitching velocity to the normal-acceleration input command for the closed-loop system. Thus,

$$\frac{\dot{\theta}}{n_i} = \frac{\frac{\theta}{\delta}\frac{n_o}{n_i}}{\frac{n_o}{\delta}} p$$

The frequency-response data determined for δ/n_i and $\dot{\theta}/n_i$ were also fed into the Fourier synthesizer to establish the transient-response characteristics of these output quantities in terms of the input normal-acceleration command.

A block diagram of the automatic control system used when the normal-acceleration command system controlled the flight path of the airplane is presented in the analysis. The closed-loop transfer function of this system is

$$\frac{\gamma_o}{\gamma_i} = \frac{K_{\gamma_\epsilon} \frac{n_o}{n_i} \frac{\gamma}{n}}{1 + K_{\gamma_\epsilon} \frac{n_o}{n_i} \frac{\gamma}{n}}$$

The transfer function relating flight-path angle to normal acceleration in the above closed-loop frequency response was determined by using equation (3). Thus,

$$\frac{\gamma}{n} = \frac{g}{Vp}$$

The transfer function relating elevator deflection to the flight-path-angle input command of the closed-loop system was obtained from the airplane transfer functions relating flight-path angle to normal acceleration and normal acceleration to elevator deflection and from the closed-loop transfer function of the system relating flight-path-angle output to the flight-path-angle input command. Thus,

$$\frac{\delta}{\gamma_i} = \frac{\frac{\gamma_o}{\gamma_i}}{\frac{\gamma_o}{n} \frac{n}{\delta}}$$

In a similar manner, the airplane transfer function relating flight-path angle to normal acceleration and the closed-loop transfer function of the system relating flight-path-angle output to flight-path-angle input command were used to establish the transfer function relating normal acceleration to the flight-path-angle input command. Thus,

$$\frac{n}{\gamma_i} = \frac{\gamma_o/\gamma_i}{\gamma_o/n}$$

The frequency-response data determined for γ_o/γ_i, δ/γ_i, and n/γ_i, when the normal-acceleration airplane-autopilot combination was used to control the flight path, were also fed into the Fourier synthesizer to establish the transient-response characteristics of these output quantities in terms of the flight-path-angle input command.

Similar transfer functions relating the pertinent variables when controlling the flight path with the pitch-attitude command system of reference 1 can be obtained by replacing the normal-acceleration transfer functions appearing in the equations presented in the preceding paragraphs with the corresponding pitch-attitude transfer functions which are presented in reference 1.

REFERENCES

1. Stokes, Fred H., and Matthews, J. T.: Theoretical Investigation of the Longitudinal Response Characteristics of a Swept-Wing Fighter Airplane Having a Pitch-Attitude Control System. NACA TN 2882, 1953.

2. Brown, Gordon S., and Campbell, Donald P.: Principles of Servomechanisms. John Wiley & Sons, Inc., 1948.

3. Seamans, R. C., Jr., Blasingame, B. P., and Clementson, G. C.: The Pulse Method for the Determination of Aircraft Dynamic Performance. Jour. Aero. Sci., vol. 17, no. 1, Jan. 1950, pp. 22-38.

TABLE I.- AIRPLANE CHARACTERISTICS, FLIGHT CONDITIONS, AND STABILITY PARAMETERS

Symbol	Condition			
	I	II	III	IV
M	0.5	0.7	0.7	0.9
h_p, ft	35,000	0	35,000	35,000
W, lb	15,291	15,291	15,291	15,291
S, sq ft	288	288	288	288
b, ft	37.1	37.1	37.1	37.1
V, ft/sec	485	779	682	877
$\bar{c}$, ft	8.085	8.085	8.085	8.085
Λ, deg	35.23	35.23	35.23	35.23
K_Y	0.95	0.95	0.95	0.95
I_Y	29,448	29,448	29,448	29,448
$l/\bar{c}$	2.4	2.4	2.4	2.4
C_L	0.611	0.0735	0.312	0.189
A	4.79	4.79	4.79	4.79
μ	277.24	85.807	277.24	277.24
C_{m_δ}	-0.427	-0.398	-0.398	-0.344
$C_{m_{C_L}}$	-0.100	-0.152	-0.126	-0.175
C_{L_δ}	0.174	0.162	0.162	0.140
C_{L_α}	4.355	4.928	4.584	6.016
C_{m_α}	-0.435	-0.751	-0.579	-1.054
$C_{m_{\alpha t}}$	-0.791	-0.825	-0.825	-0.848
$C_{L_{\alpha t}}$	0.323	0.337	0.337	0.346
$C_{L_{D\theta}}$	0.791	0.825	0.825	0.848
$C_{m_{D\theta}}$	-1.897	-2.017	-2.017	-2.074
$C_{L_{D\alpha}}$	0.1583	0.272	0.404	0.392
$C_{m_{D\alpha}}$	-0.3876	-0.664	-0.991	-0.962
$d\epsilon/d\alpha$	0.35	0.395	0.368	0.483

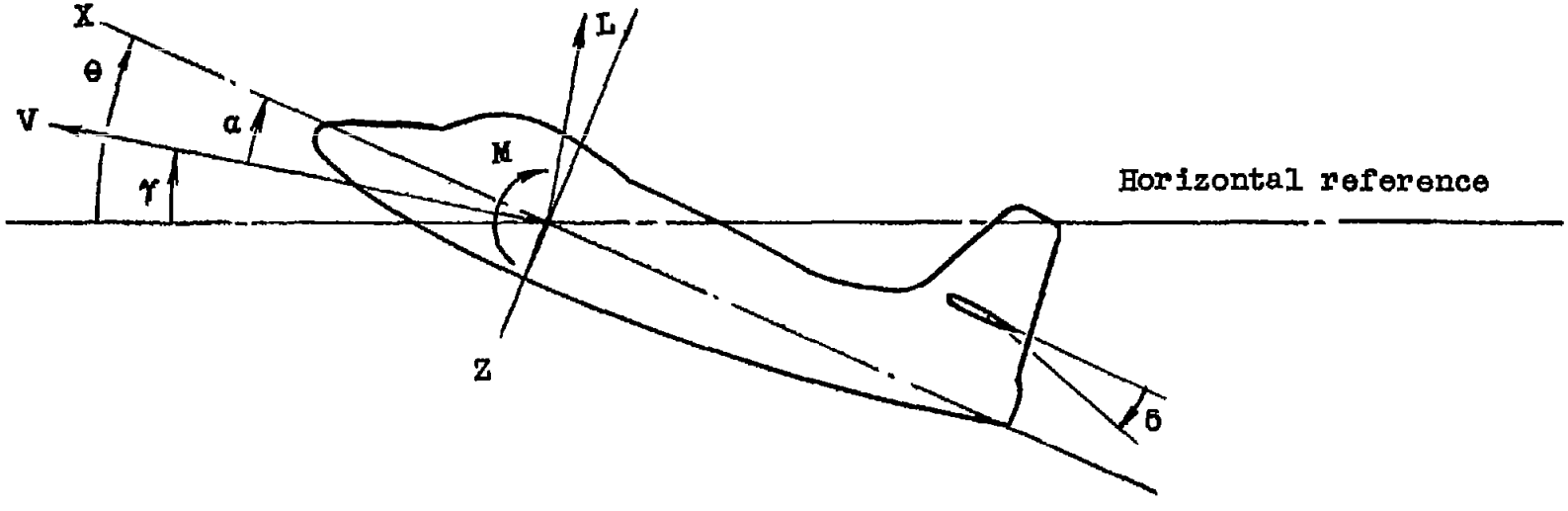

Figure 1.- System of axes and angular relationship in flight. Arrows indicate positive direction.

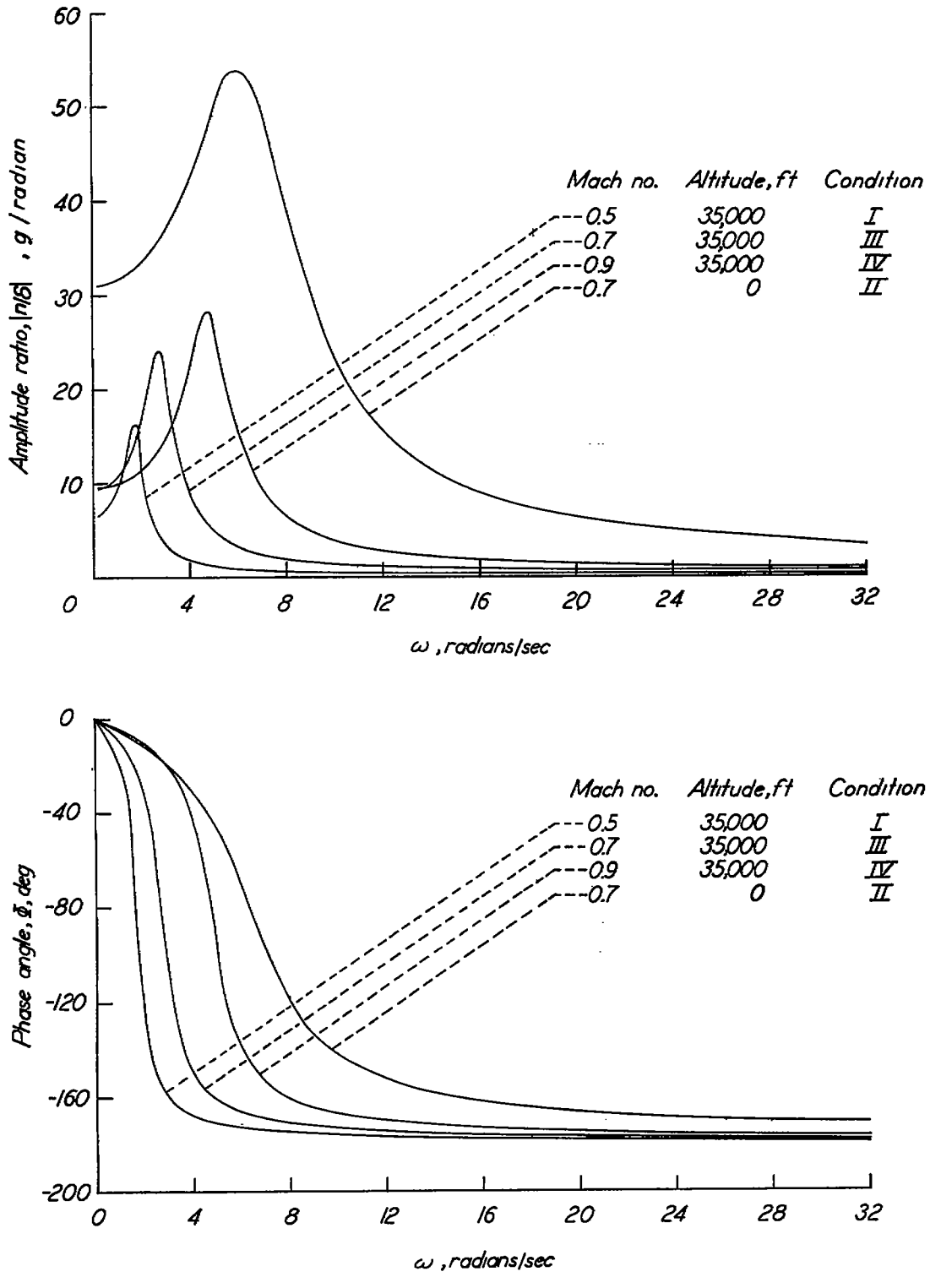

Figure 2.- Airplane frequency response.

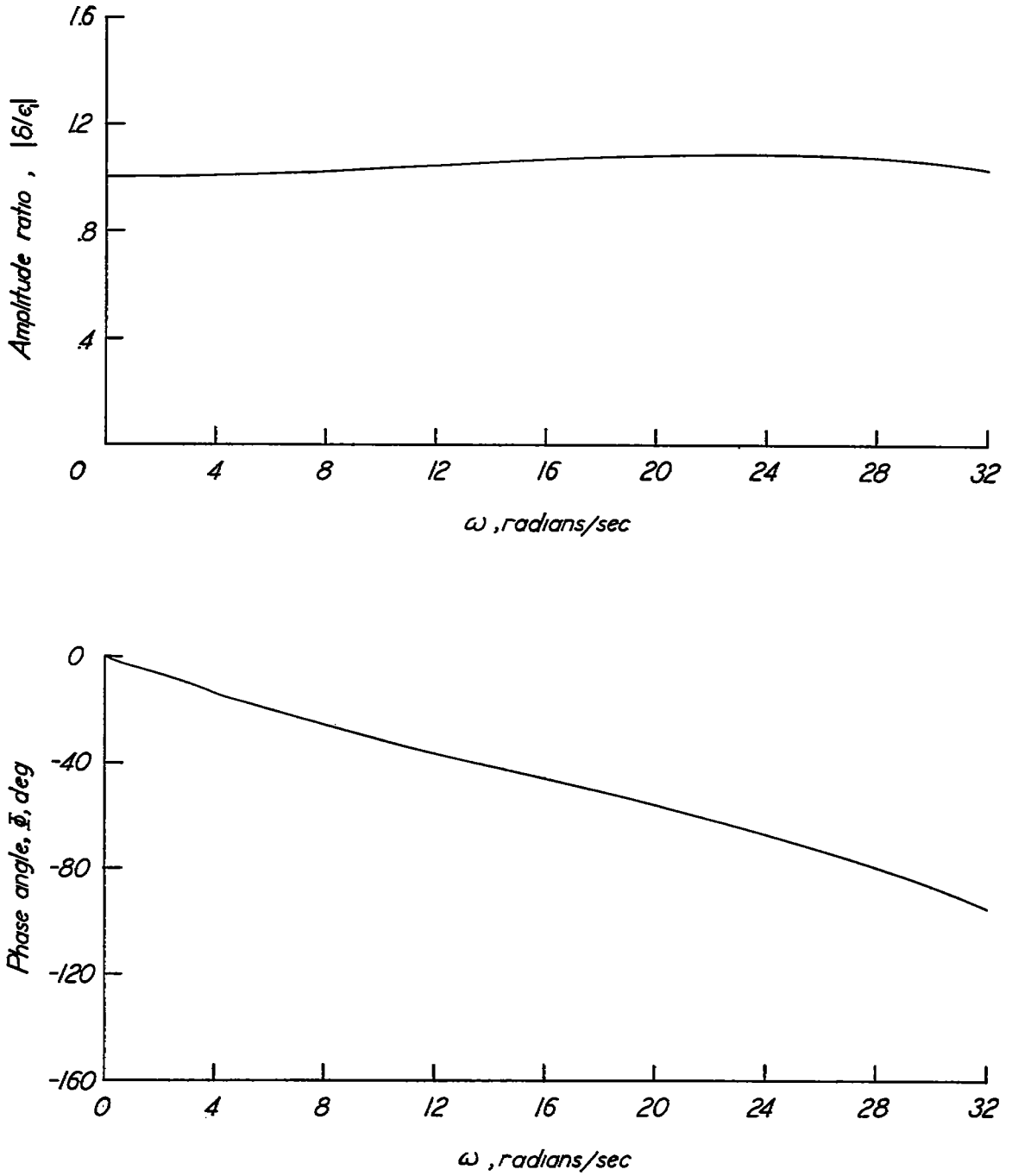

Figure 3.- Elevator-servocontrol-system frequency response.

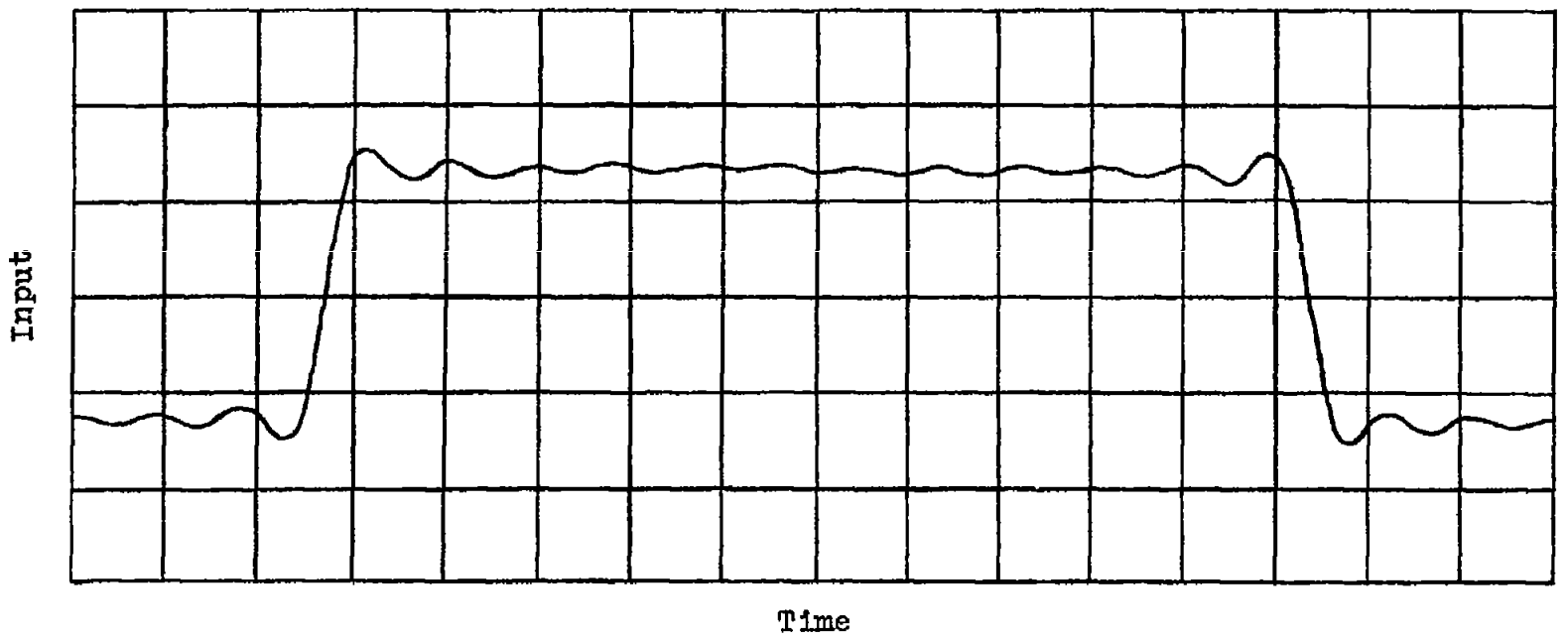

Figure 4.- Approximate square-wave input produced by Fourier synthesizer.

Parameter settings	Frequency response	Transient response	Response characteristics
K_{n_ϵ}=0.08	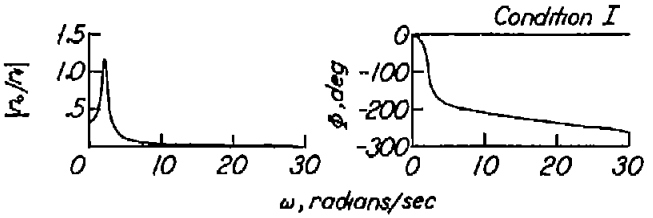	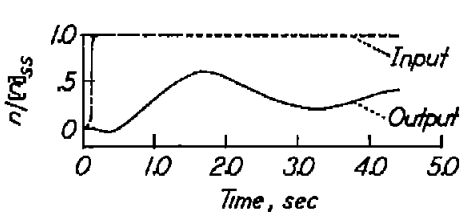	ω_p =2.0 radians/sec T_R = — $C_{1/2}$=0.56 cycles ϵ_{ss}= 67.0%
K_{n_ϵ}=0.02	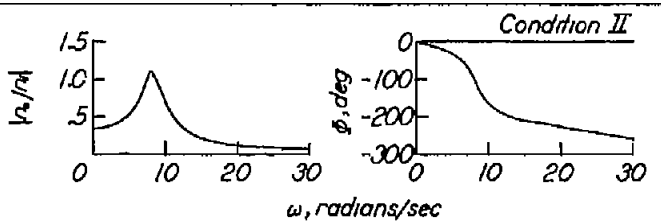	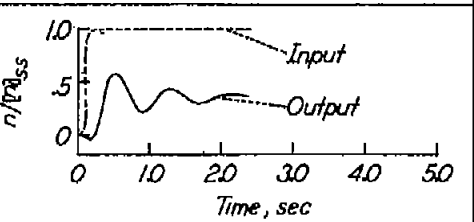	ω_p =8.6 radians/sec T_R =2.8 sec $C_{1/2}$=0.71 cycles ϵ_{ss}= 65.0%
K_{n_ϵ}=0.05	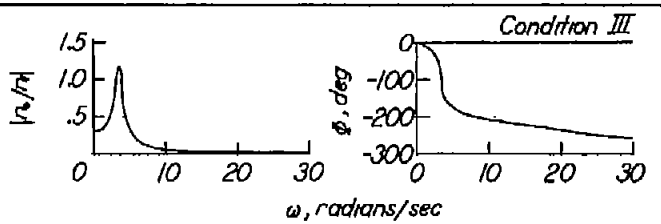	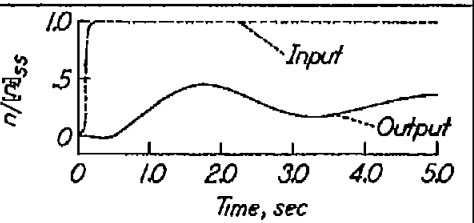	ω_p =3.5 radians/sec T_R =10.0 sec $C_{1/2}$=0.83 cycles ϵ_{ss}= 69.0%
K_{n_ϵ}=0.03	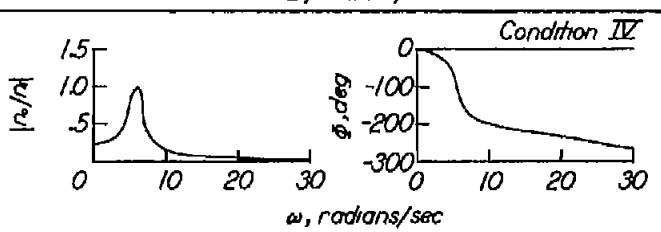	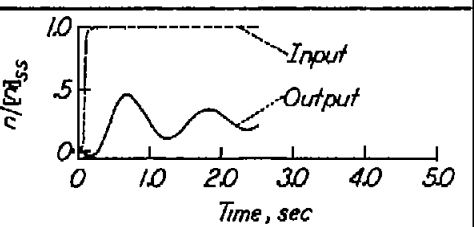	ω_p =5.5 radians/sec T_R =5.0 sec $C_{1/2}$=1.00 cycles ϵ_{ss}= 77.0%

Figure 5.- Frequency and transient responses of airplane-autopilot combination without rate gyro or lag network for conditions I, II, III, and IV.

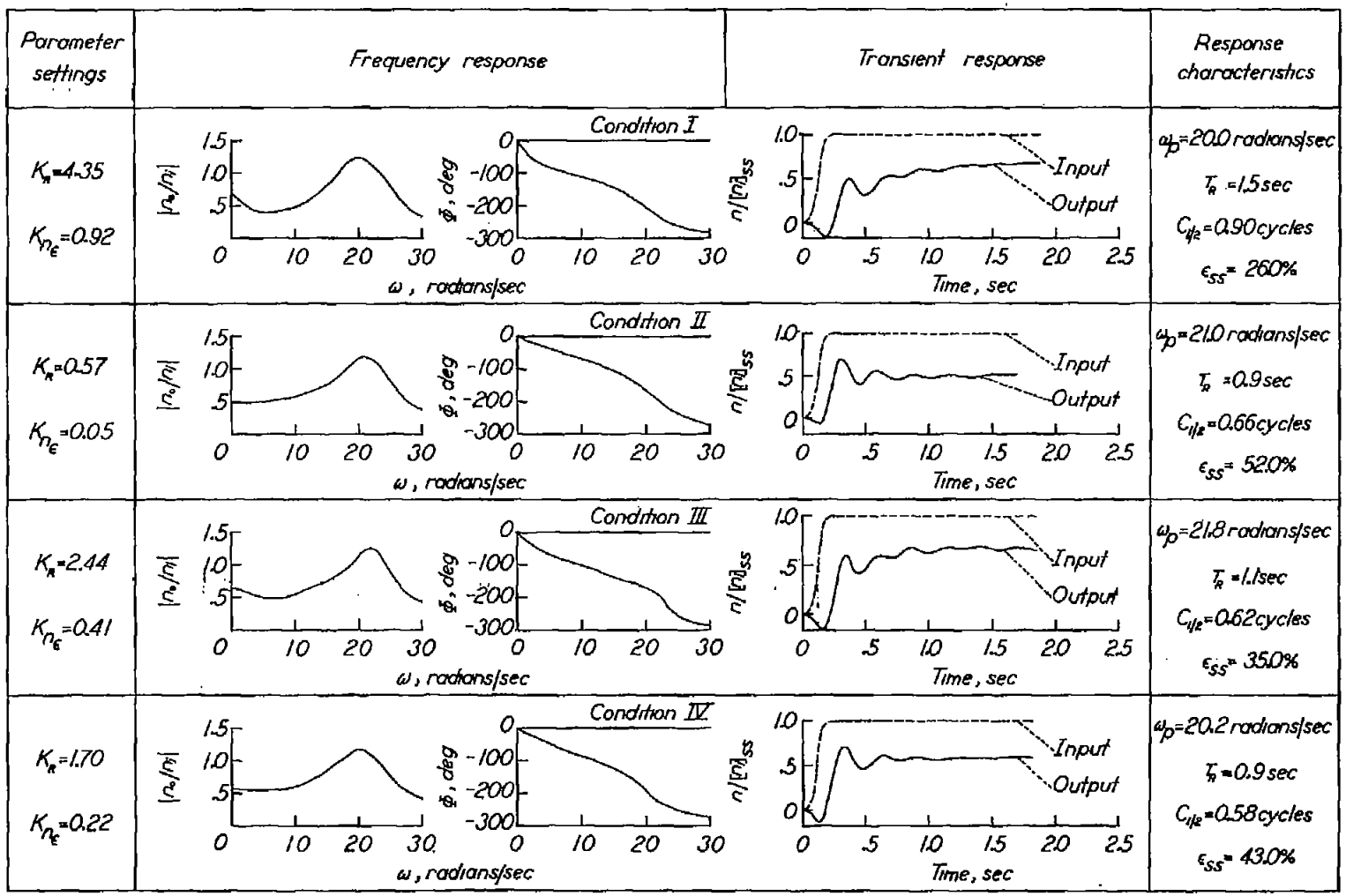

Figure 6.- Frequency and transient responses of airplane-autopilot combination with rate gyro without lag network for conditions I, II, III, and IV.

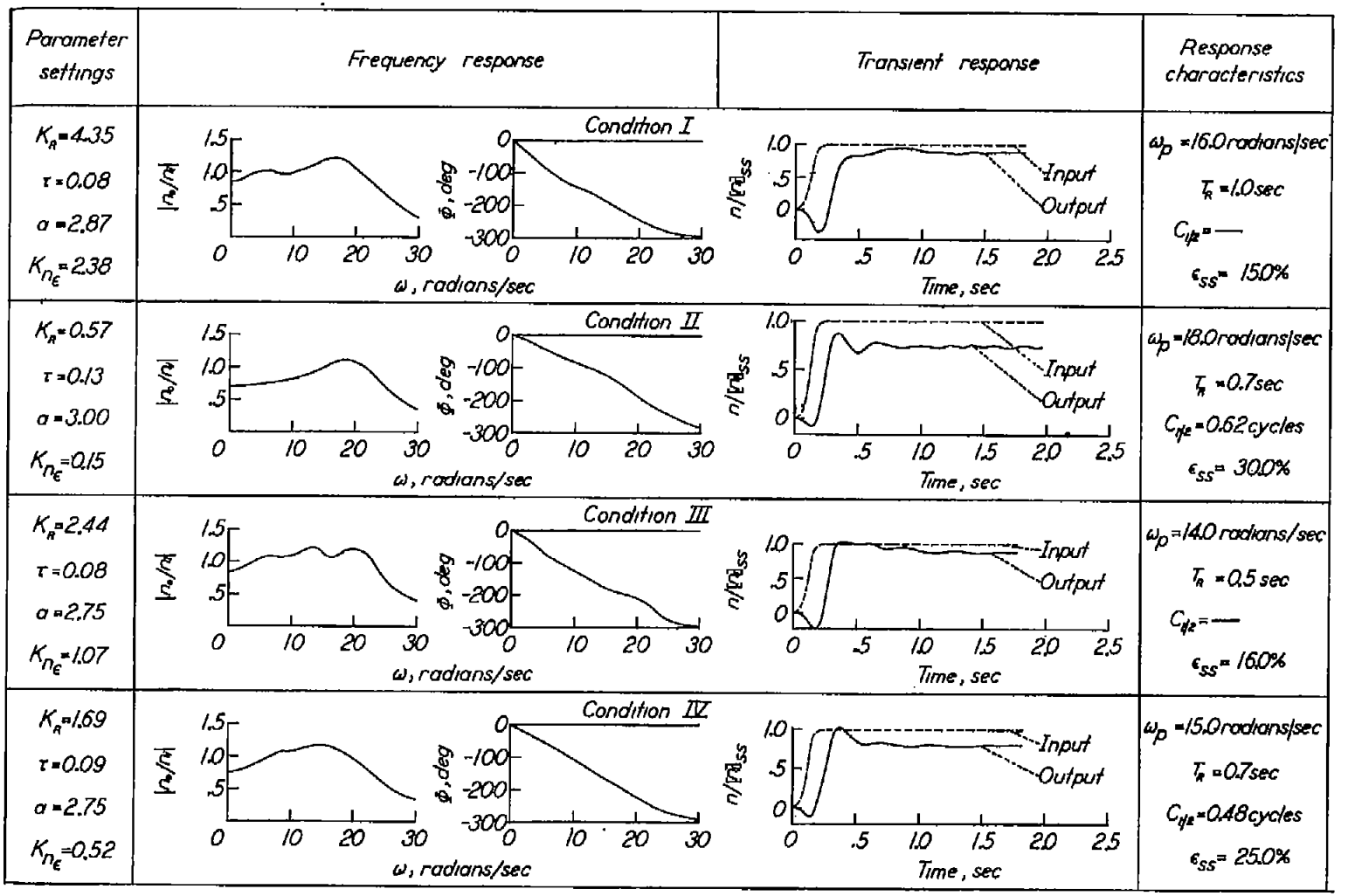

Figure 7.- Frequency and transient responses of airplane-autopilot combination with both rate gyro and lag network when best parameter settings obtained at each condition are used.

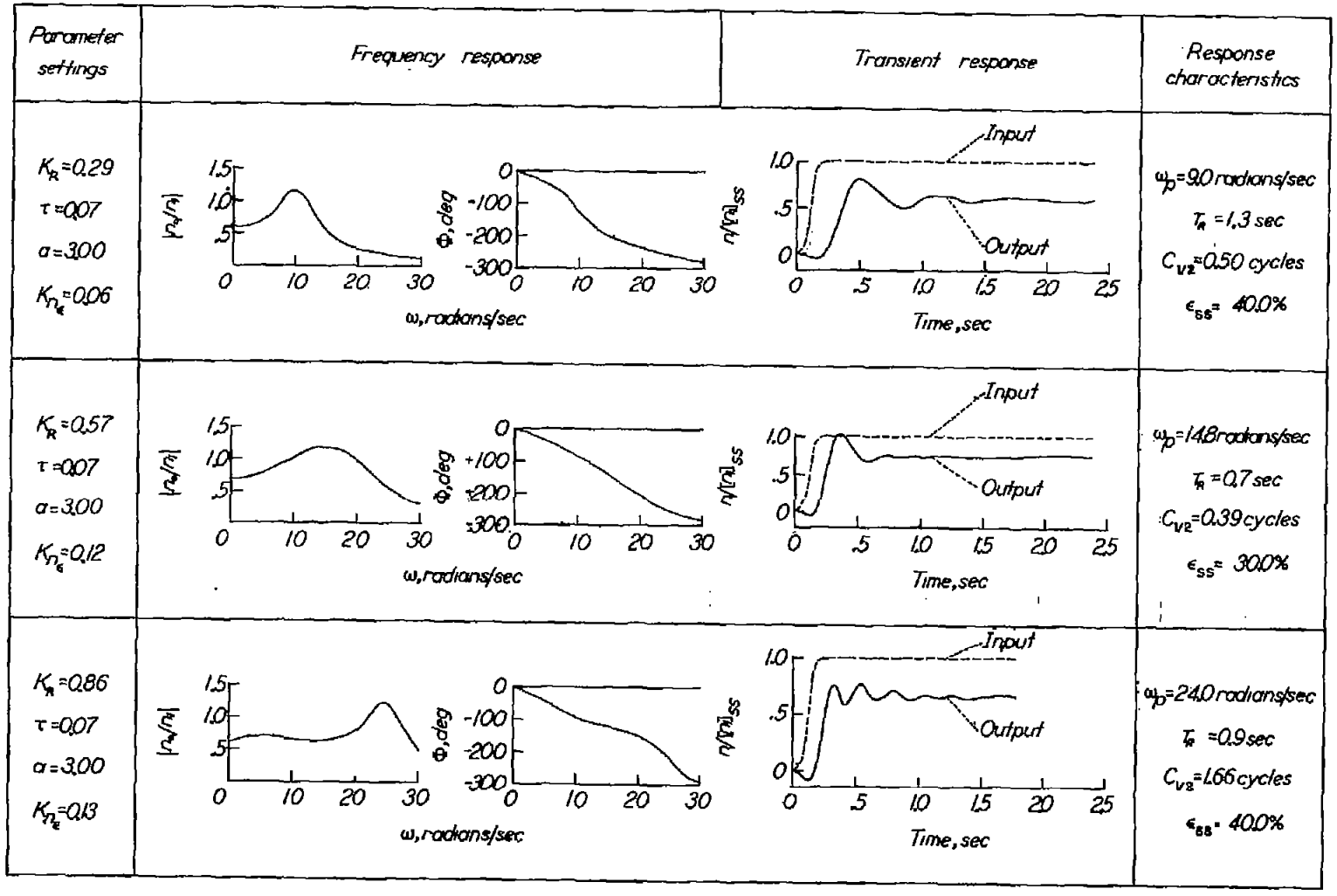

Figure 8.- Effects of rate gain settings K_R upon frequency and transient responses of airplane-autopilot combination with both rate gyro and lag network. Condition II (M = 0.7; h_p = 0).

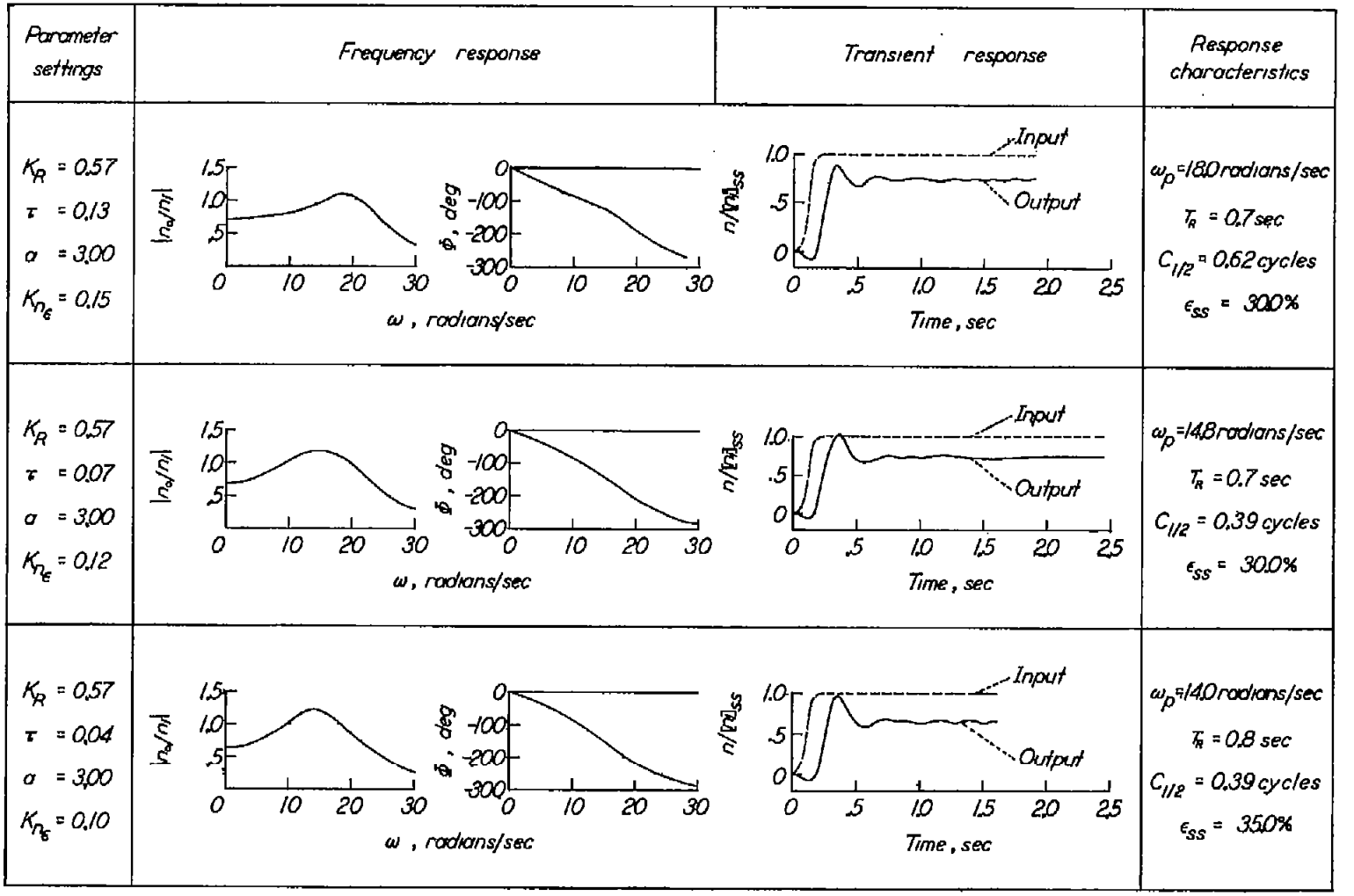

Figure 9.- Effects of integrator time constant τ upon frequency and transient responses of airplane-autopilot combination with both rate gyro and lag network. Condition II (M = 0.7; h_p = 0).

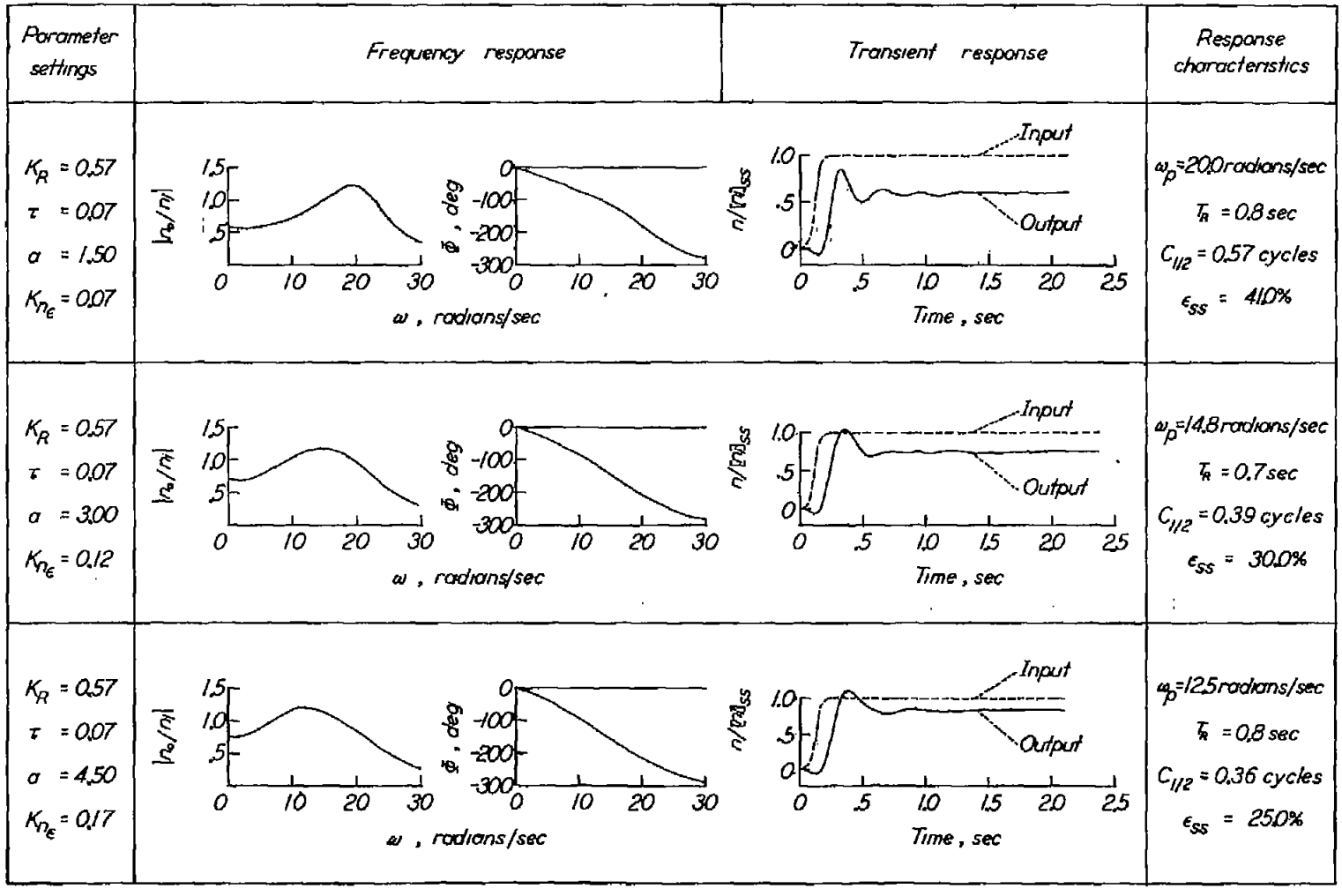

Figure 10.- Effects of integrator time constant a upon frequency and transient responses of airplane-autopilot combination with both rate gyro and lag network. Condition II (M = 0.7; h_p = 0).

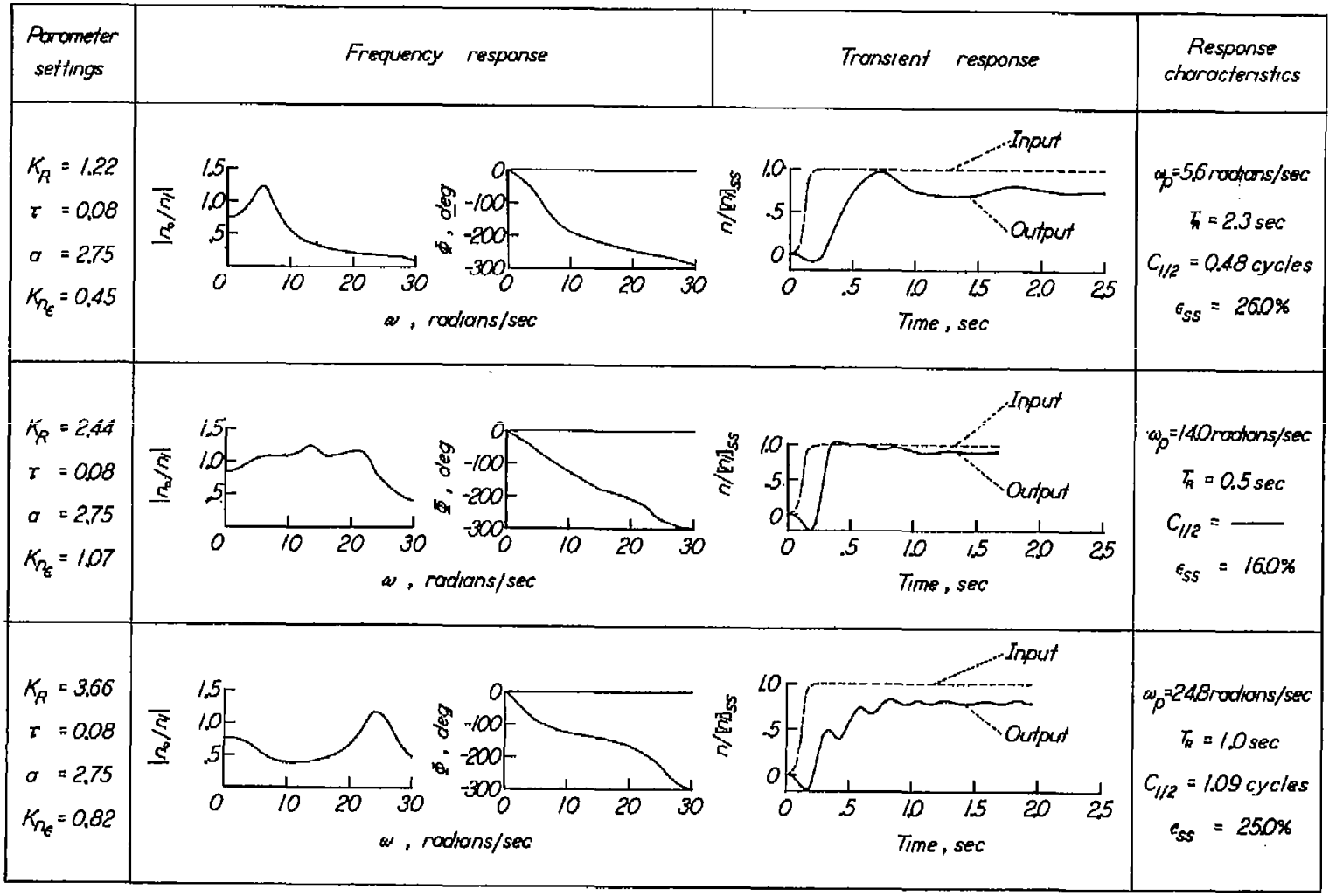

Figure 11.- Effects of rate gain settings K_R upon frequency and transient responses of airplane-autopilot combination with both rate gyro and lag network. Condition III (M = 0.7; h_p = 35,000 feet).

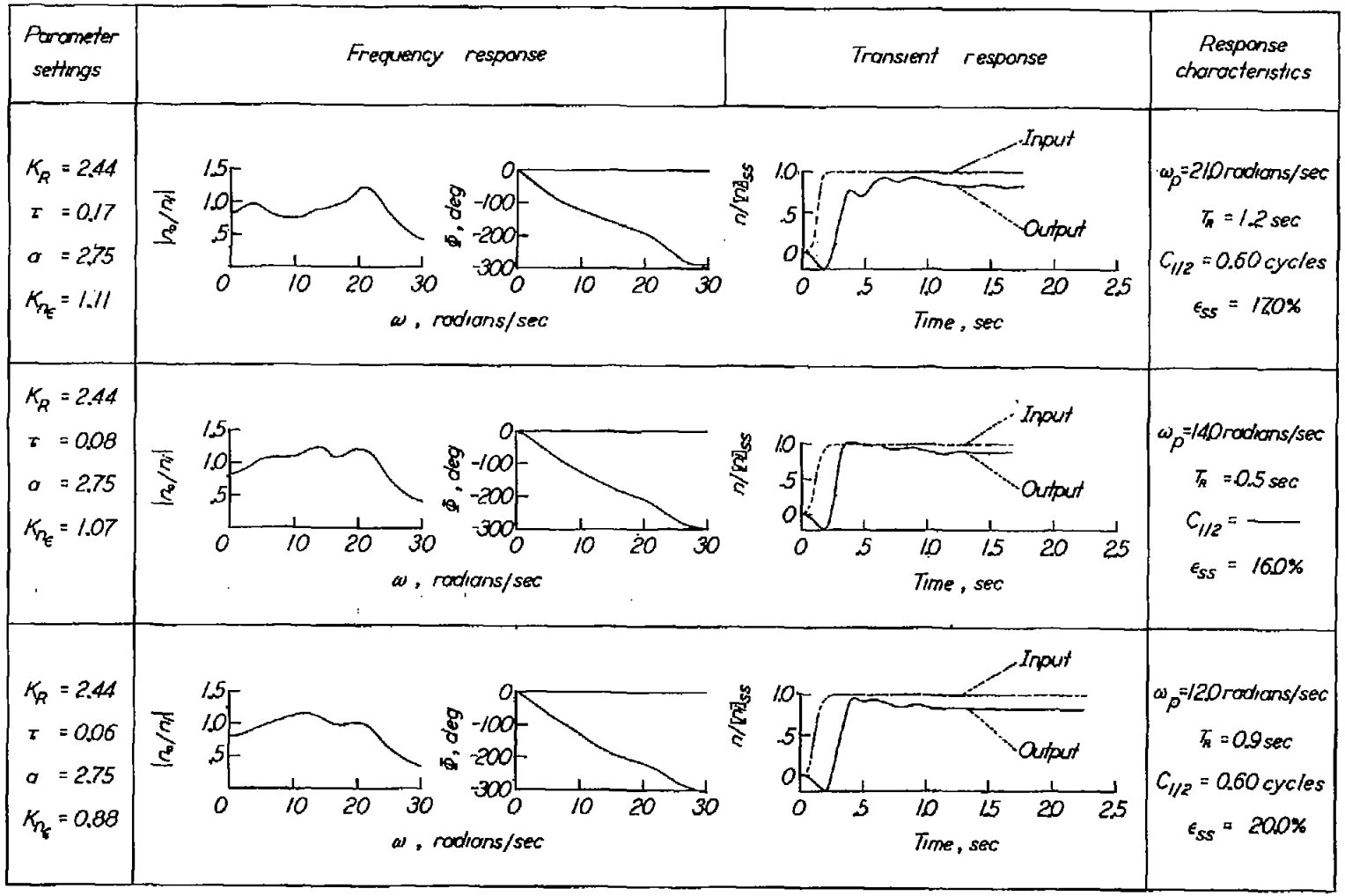

Figure 12.- Effects of lag-network time constant τ upon frequency and transient responses of airplane-autopilot combination with both rate gyro and lag network. Condition III (M = 0.7; h_p = 35,000 feet).

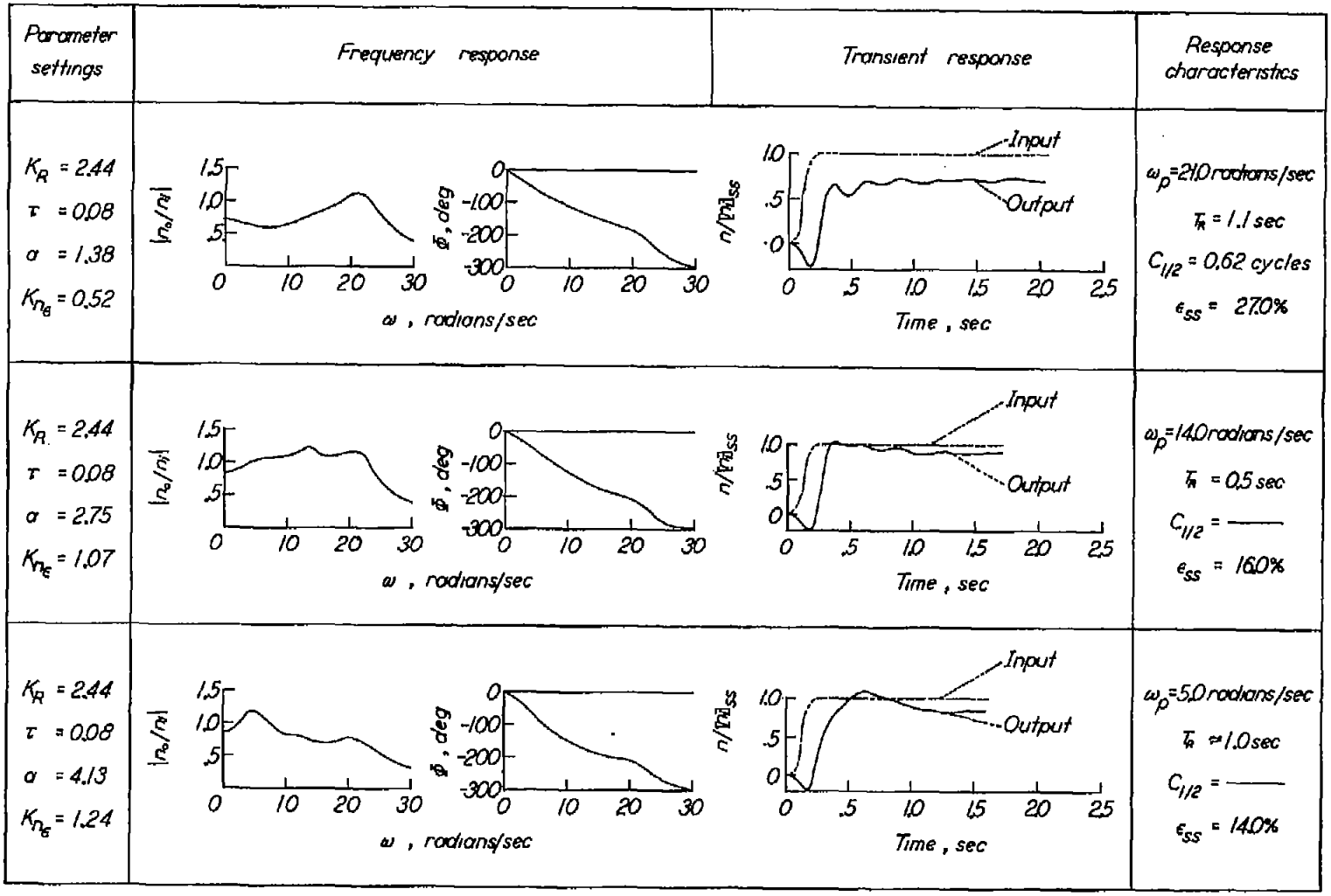

Figure 13.- Effects of integrator time constant ratio a upon frequency and transient responses of airplane-autopilot combination with both rate gyro and lag network. Condition III (M = 0.7; h_p = 35,000 feet).

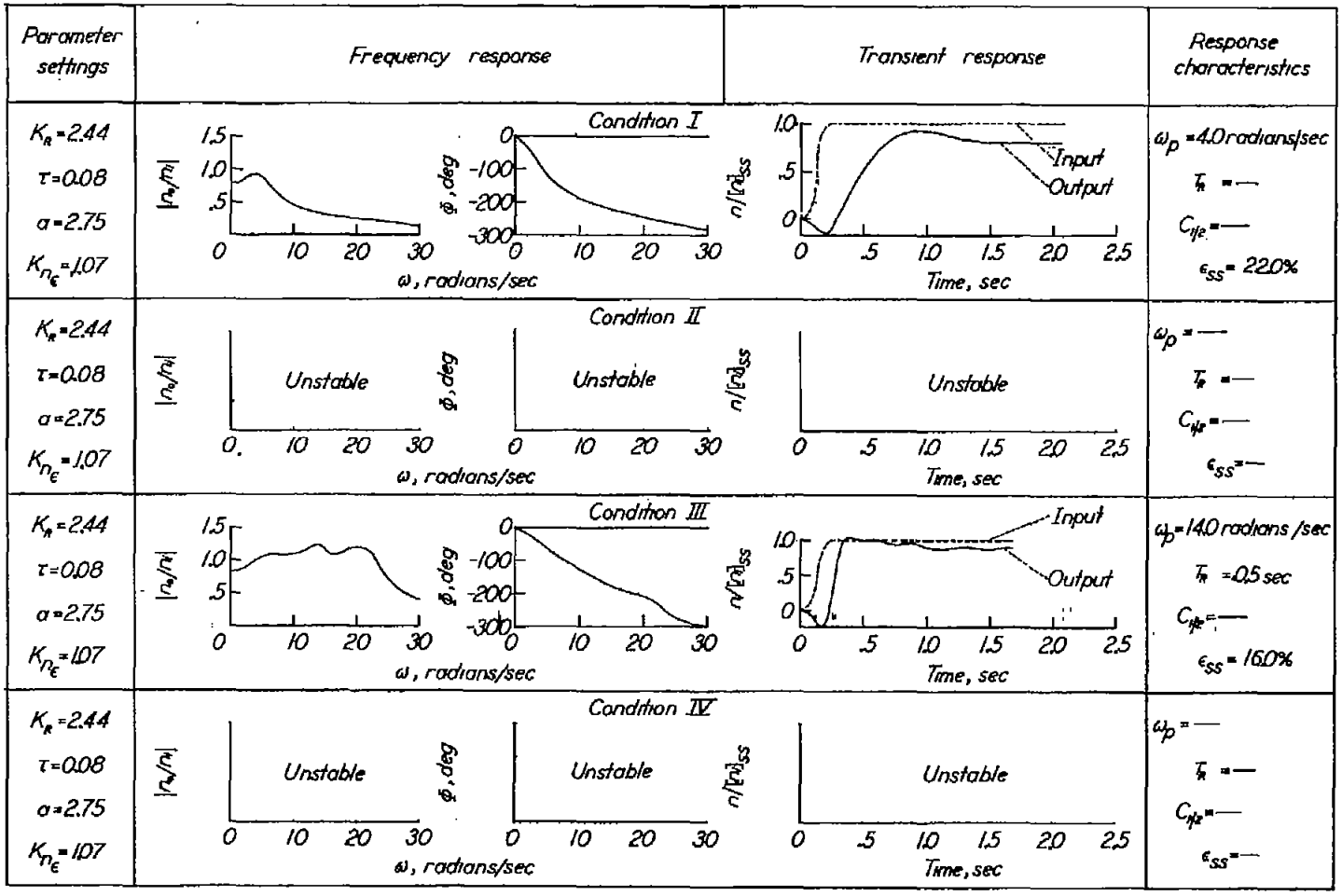

Figure 14.- Frequency and transient responses of airplane-autopilot combination with both rate gyro and lag network when best parameter settings obtained at condition III (M = 0.7; h_p = 35,000 feet) are used.

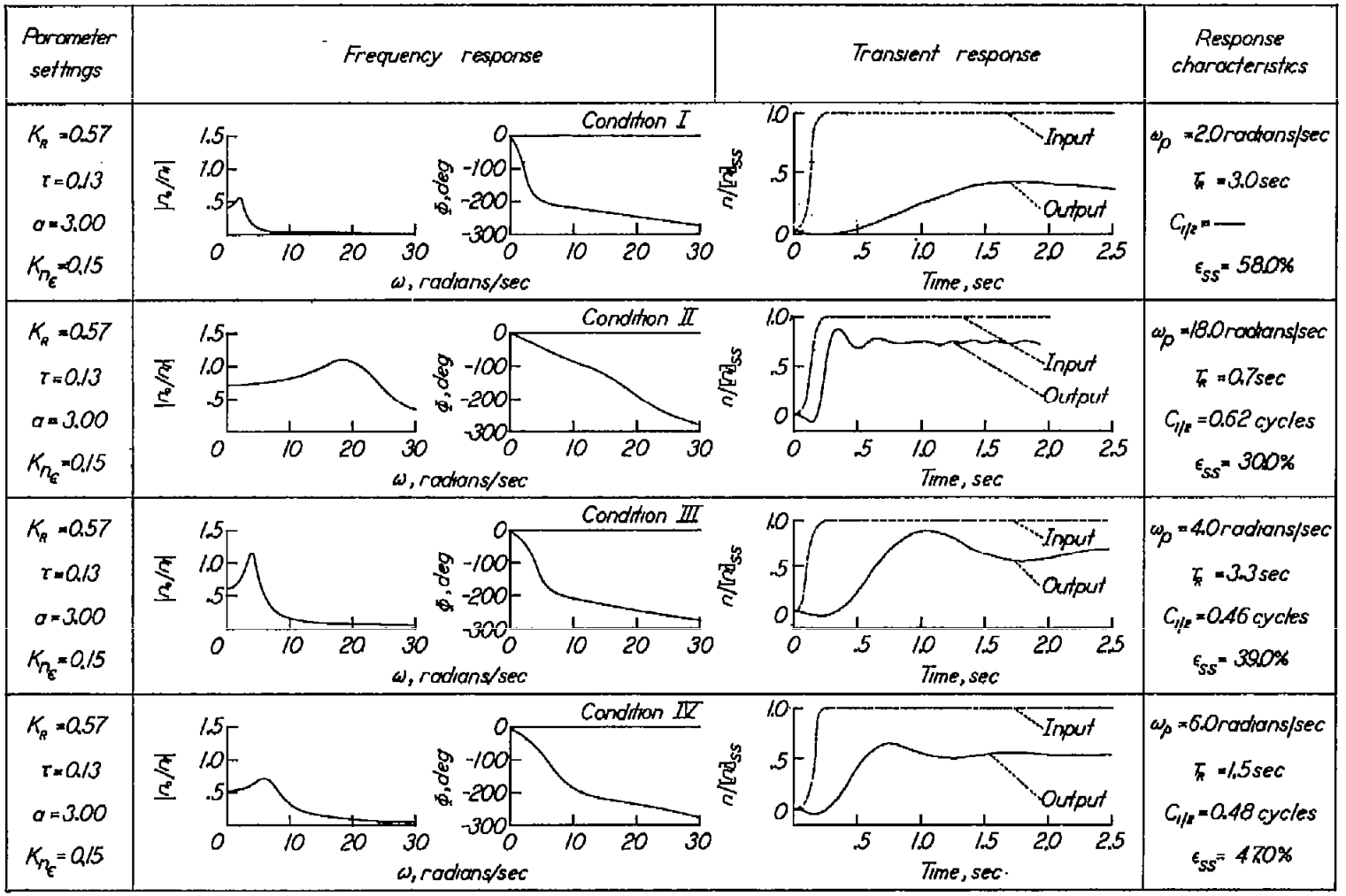

Figure 15.- Frequency and transient responses of airplane-autopilot combination with both rate gyro and lag network when best parameter settings obtained at condition II (M = 0.7; h_p = 0) are used.

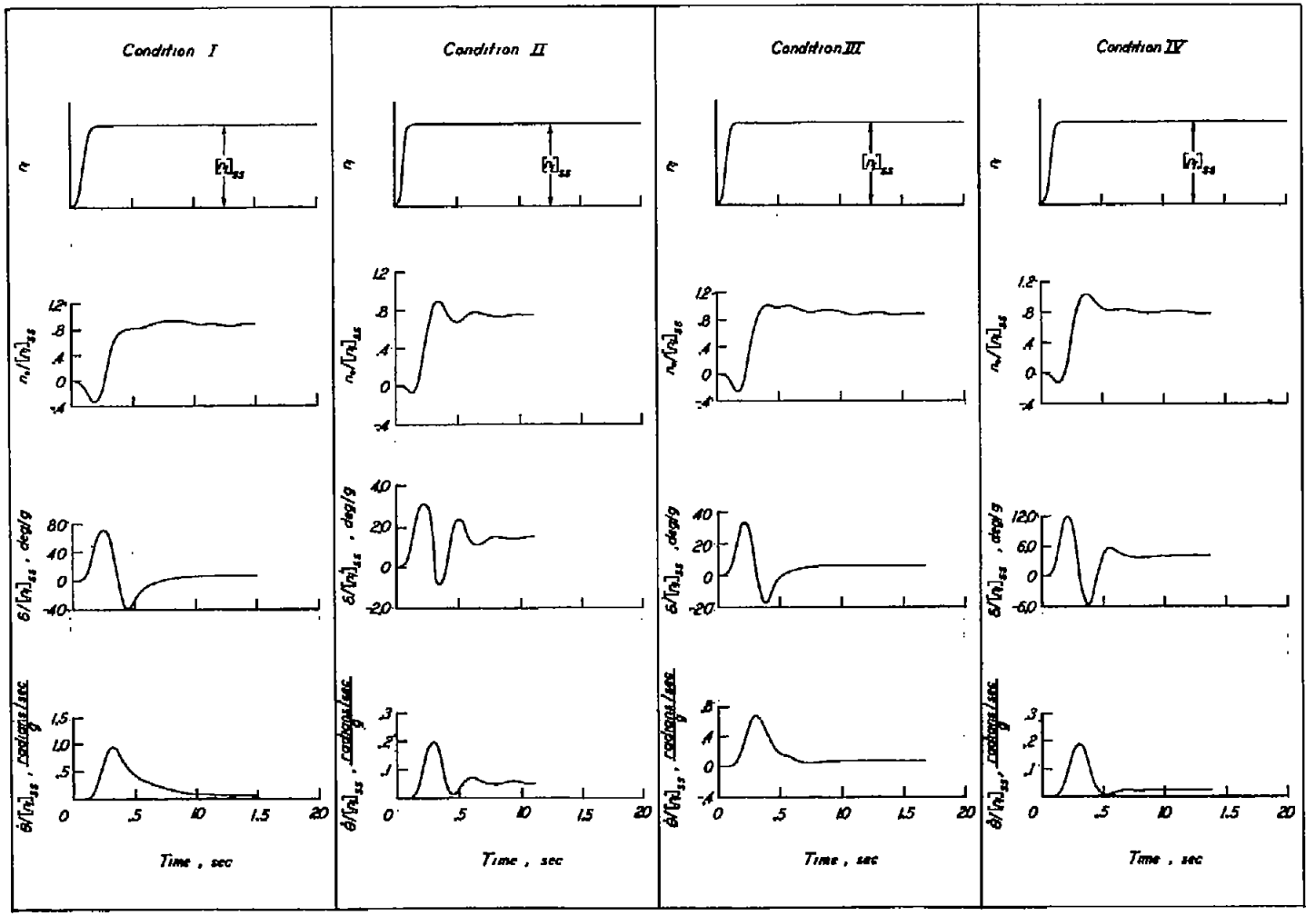

Figure 16.- Responses in normal acceleration, elevator deflection, and pitching velocity to normal-acceleration command when best parameter settings obtained at each condition are used.

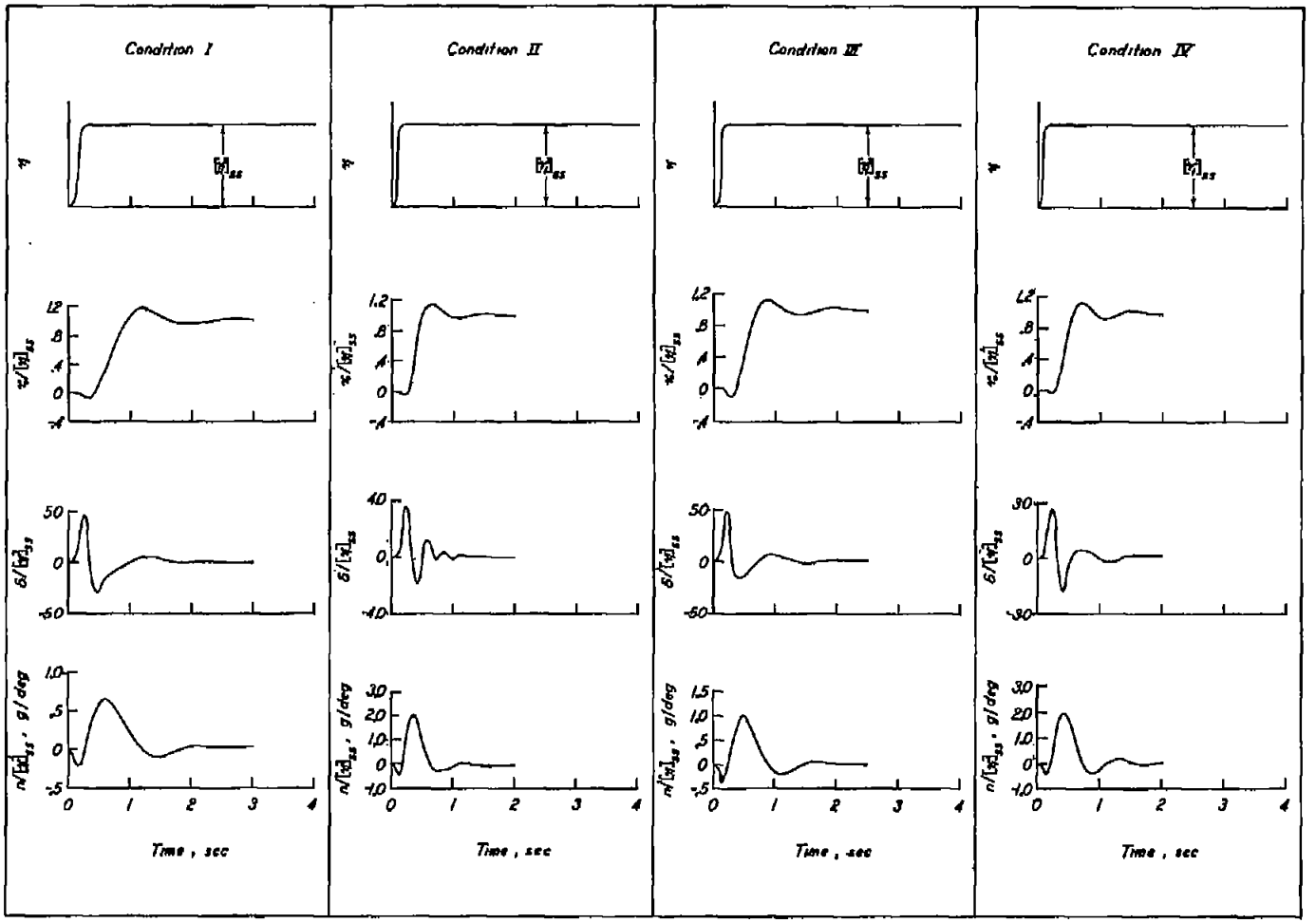

Figure 17.- Responses in flight path, elevator deflection, and normal acceleration to flight-path command when normal-acceleration system is utilized as an inner loop. Best parameter settings are used for each condition.

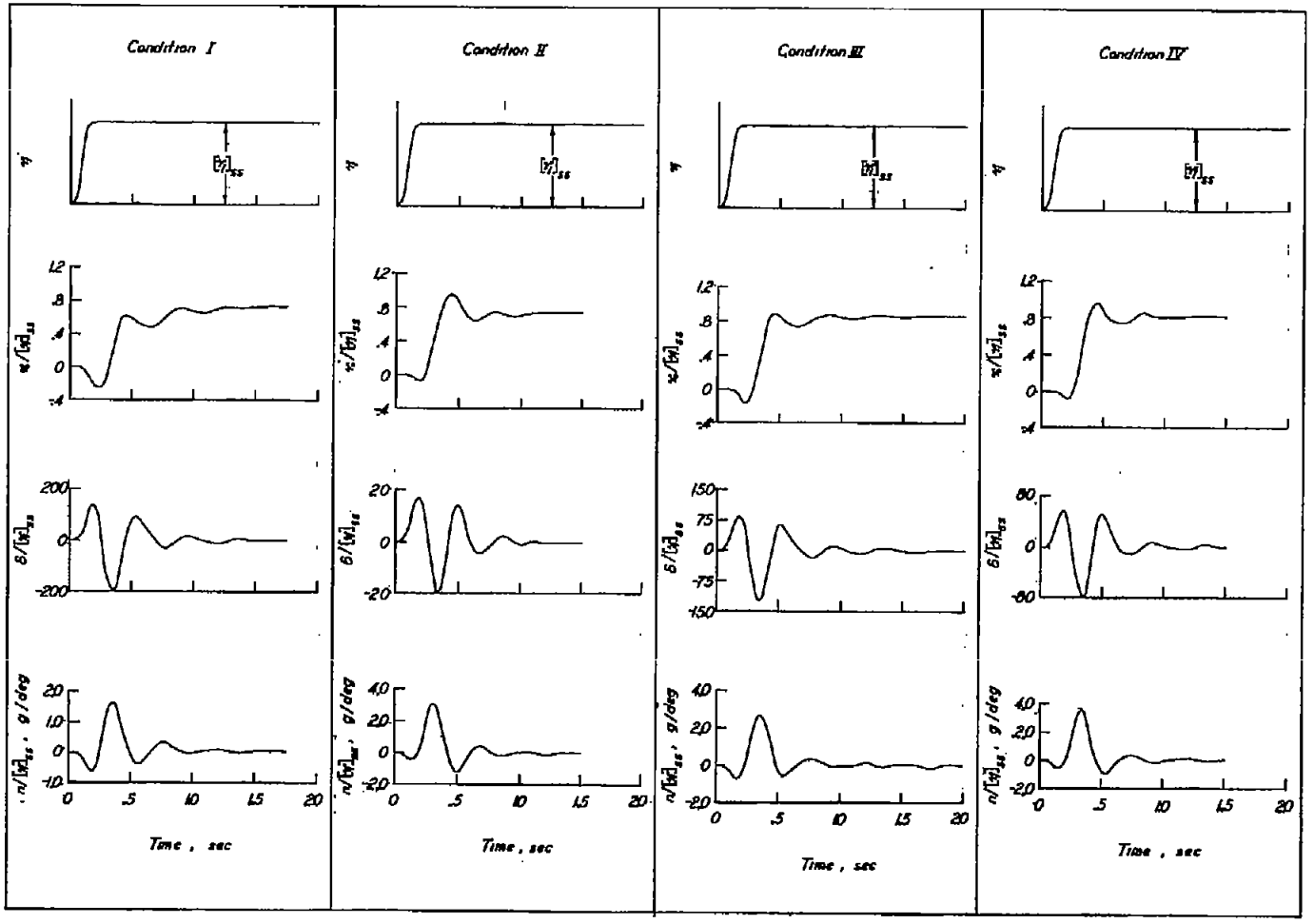

Figure 18.- Responses in flight path, elevator deflection, and normal acceleration to flight-path command when pitch-attitude system (ref. 1) is utilized as an inner loop. Best parameter settings are used for each condition.

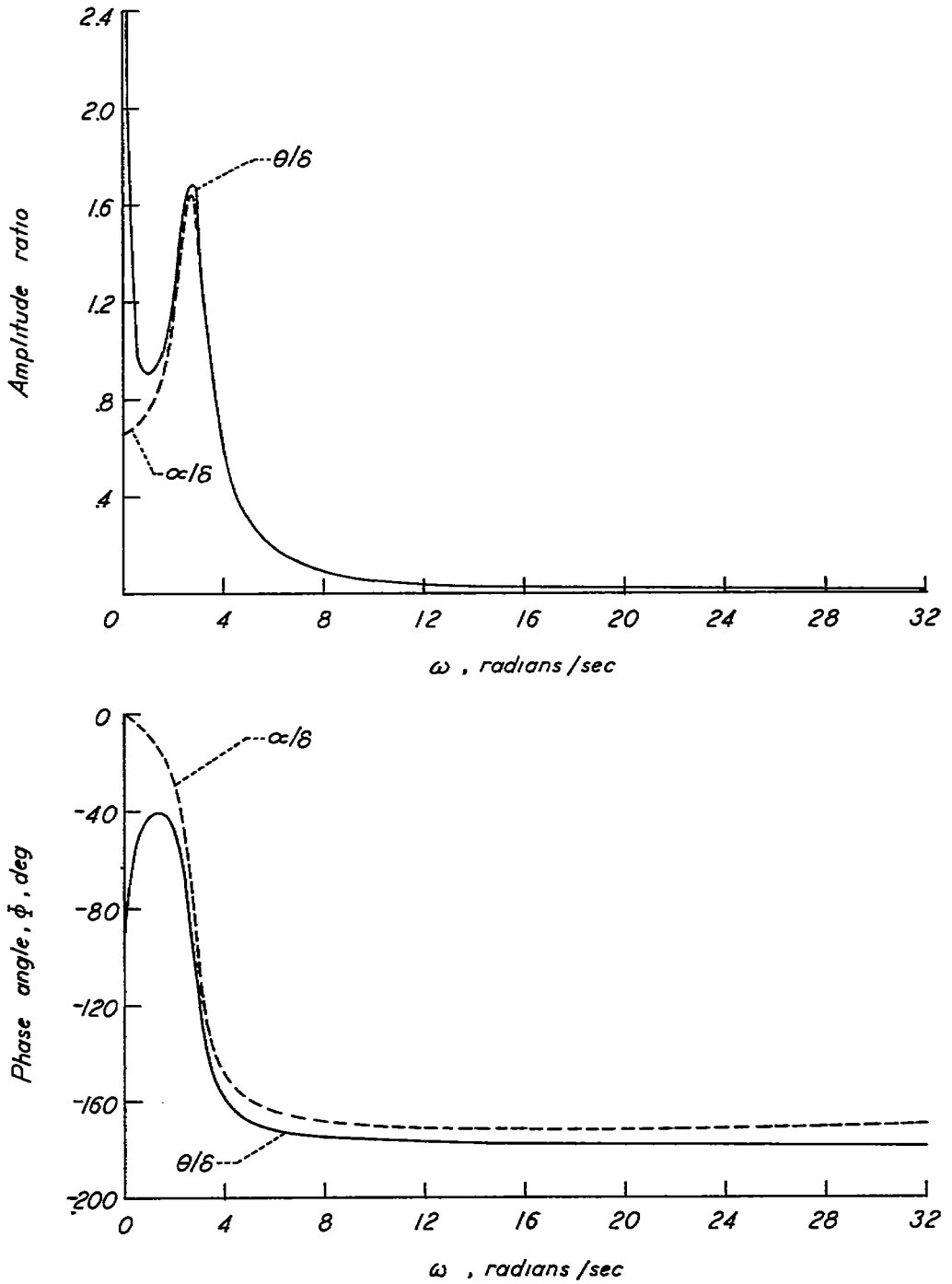

Figure 19.- Comparison of airplane transfer functions relating pitch attitude and angle of attack to elevator deflection. Condition III (M = 0.7; h_p = 35,000 feet).

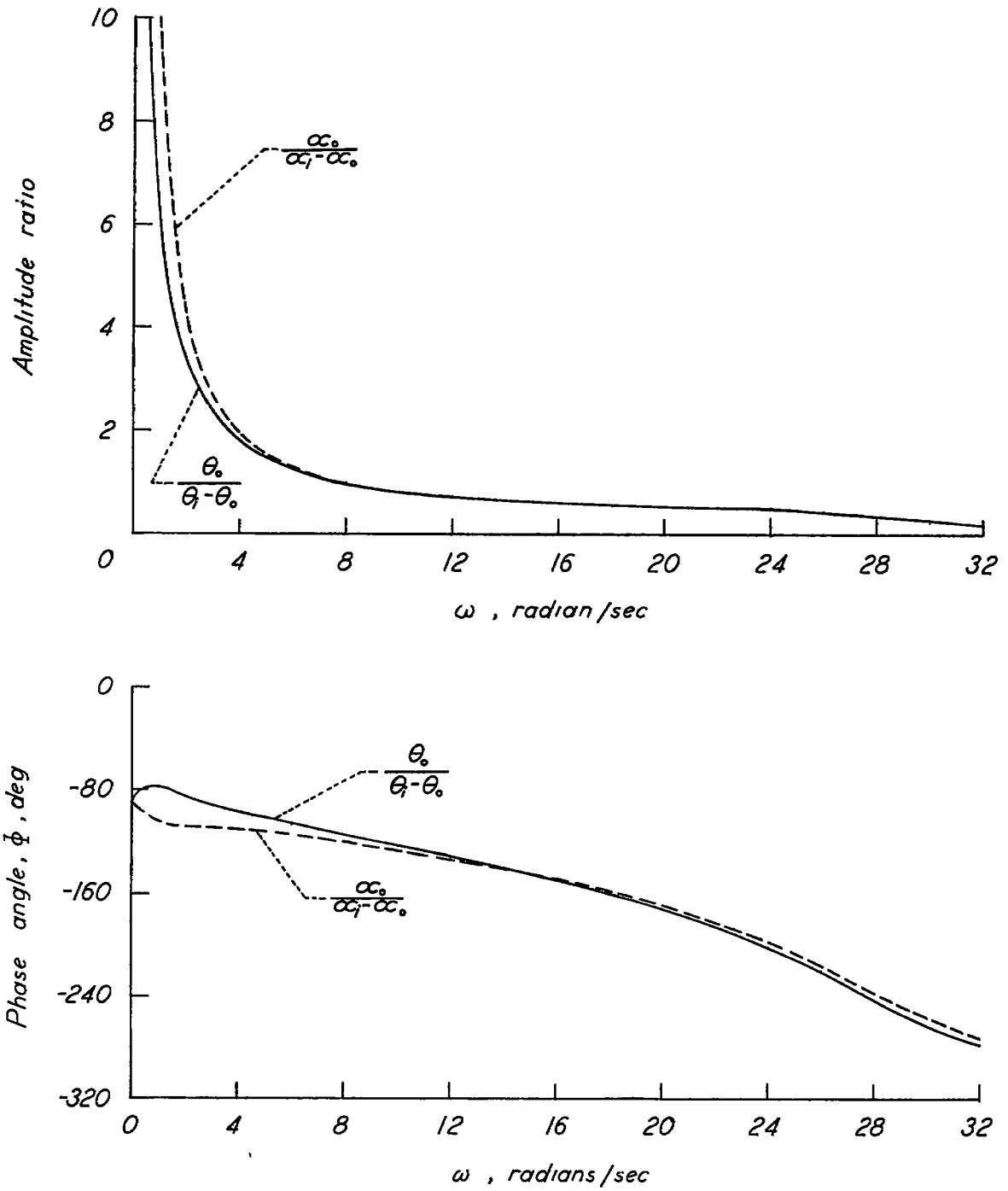

Figure 20.- Comparison of open-loop transfer function of airplane-autopilot combination used for control of pitch attitude with that used for control of angle of attack. Lag network incorporated in angle-of-attack system. Condition III (M = 0.7; h_p = 35,000 feet).

NACA-Langley - 7-9-54 - 1000